INSTITUT d'OPTIQUE GRADUATE SCHOOL ParisTech | LEnsE Laboratoire d'Enseignement Expérimental

Lab work in photonics
Quantum photonics

Salles	**P1**	**P2**	**P3**	**P4**	**P5**
	N1.6	S1.29	N1.3	R1.61	R1.57

lense.institutoptique.fr / Troisième année/ Photonique 3A|M2

Engineer - 3rd year - Palaiseau

Master 2 QLMN
Year 2023-2024

P 1

Entangled photons and Bell's inequality

Questions P1 to P11 have to be done before the class.

Contents

1 Introduction

Quantum theory does not allow one to calculate the outcome of a measurement, but rather the probability of the different possible outcomes. Because of this probabilistic aspect, many physicist, including Einstein, were dubious and thought that quantum mechanics had to be an incomplete theory that was not accounting for the full reality. To illustrate this point, Einstein, Podolski and Rosen presented in 1935 a "gedankenexperiment" (mental experiment) where a measurement on an entangled two-particle state (Bell state or EPR state) lead to a paradox, which the authors interpret as a proof of the incompleteness of the quantum theory [1].

For a Bell state, a measurement of the state of each particle taken individually gives a random outcome, but the results on the two particles are perfectly correlated. In other words, a measurement of the first particle state allows us

[1] A. Einstein, B. Podolsky et N. Rosen, *Can Quantum-Mechanical Description of Physical Reality Be Considered Complete?*, Physical Review **47**, 777 (1935)

to predict with certainty the state of the second one. For Einstein, Podolsky and Rosen, the possibility of predicting the state of the second particle implies that this state exists before the measurement, implying that there is a set of "hidden" variables (in the sense that they are not described by the theory) that determine this state all along the experiment.

For a long time, it has seemed that the debate between an hidden variable interpretation and a purely probabilistic theory was a philosophical discussion. However, in 1964, John Bell [2] showed that there were some cases where the two interpretations were leading to incompatible observations, and that it was possible to settle the debate with an experiment. But it has been necessary to wait 15 more years for the progress in **quantum optics** to implement this experiment with pairs of entangled photons. The first unambiguous results have been obtained at the Institut d'Optique by Alain Aspect, Philippe Grangier and Jean Dalibard [3].

This lab work, inspired by **M. W. Mitchell** and **D. Dehlinger**, aims to produce a two-photons Bell state, and allows you to determine, with your own measurements, which theory can be invalidated.

2 Bell states

2.1 Polarization state of a photon in quantum mechanic

When we measure the polarization of a photon with a vertical analyzer, we refer to the basis formed by the vertical polarization ($|V\rangle$ parallel to the analyzer axis) and the horizontal polarization ($|H\rangle$ orthogonal to the analyzer axis). In this basis, the polarization state is written:

$$|\psi\rangle = c_V|V\rangle + c_H|H\rangle\,. \tag{1.1}$$

The coefficients c_V and c_H are complex number such as $|c_V|^2 + |c_H|^2 = 1$. The measurement of the photon polarization can only gives two outcomes:

- The photon is transmitted by the polariser and its polarization state is projected on $|V\rangle$. Quantum mechanics predicts that the probability of this result is $P_V = |\langle\psi|V\rangle|^2 = |c_V|^2$;
- The photon is blocked by the polariser and its polarization state is projected on $|H\rangle$. The associated probability is $P_H = |\langle\psi|H\rangle|^2 = |c_H|^2$.

[2] J. S. Bell, *On the Einstein-Podolsky-Rosen paradox*, Physics **1**, 195 (1964)

[3] See for instance : A. Aspect, J. Dalibard et G. Roger, *Experimental Test of Bell's Inequalities Using Time-Varying Analyzers*, Physical Review Letters **49**, 1804 (1982)

P1 Write the polarization state of a photon with a rectilinear polarization, at an angle α from the vertical. What is the probability to measure it in the state $|V\rangle$?

P2 Write the polarization state of a photon with a left-circular polarization. What is the probability to measure it in the state $|V\rangle$?

If we choose to measure the polarization state of a photon with a polariser rotated by an angle α from the vertical, the new basis of the polarization state is $\{|V_\alpha\rangle, |H_\alpha\rangle\}$ (figure 1.1).

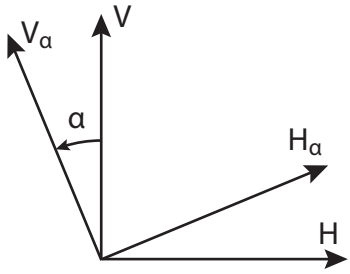

Figure 1.1: The basis of the polarization state $\{|V_\alpha\rangle, |H_\alpha\rangle\}$ is obtained by rotating the basis $\{|V\rangle, |H\rangle\}$ by an angle α.

P3 Consider a photon in the polarization state $|V\rangle$. Write its state in the basis $\{|V_\alpha\rangle, |H_\alpha\rangle\}$. What is the probability P_{V_α} of measuring the polarization V_α?

2.2 Pairs of polarization-entangled photons

During this lab work, you will produce and characterize pairs of polarization-entangled photons. The polarization state of those pairs is a Bell state, written as follow:

$$|\psi\rangle = \frac{1}{\sqrt{2}} \left(|V, V\rangle + |H, H\rangle\right) . \tag{1.2}$$

It is a non separable state, which means that we can not assign a polarization state to each photon individually.

P4 Show that the probability P_V of measuring the photon 1 **or** the photon 2 in the polarization V is 1/2.

P5 What is the probability of measuring the two photons in the same polarization state (V, V or H, H)? What is the probability of measuring the two photons in orthogonal polarization states (V, H or H, V)?

In other words, a polarization measurement on one of the photons gives a random result, but if we measure the polarizations of the two photons of the pair, the results are always **correlated**. More generally, the probability to measure simultaneously the photon 1 in the polarization state V_α and the photon 2 in the polarization state V_β is given by

$$P(V_\alpha, V_\beta) = |\langle V_\alpha, V_\beta|\psi\rangle|^2 \ . \tag{1.3}$$

P6 Show that $P(V_\alpha, V_\beta) = \cos^2(\alpha - \beta)/2$. How does this probability change when the two axis of analysis are rotated by the same angle?

P7 Show that the Bell state has the same form than (1.2) no matter what the basis of analysis is, which implies that:

$$|\psi\rangle = \frac{1}{\sqrt{2}} \left(|V_\alpha, V_\alpha\rangle + |H_\alpha, H_\alpha\rangle\right) \ , \quad \forall\alpha \, . \tag{1.4}$$

This **rotational symmetry** of the polarization state is a crucial property of the Bell state that we will use to reveal the full extent of the correlation between the entangled photons.

2.3 Bell's inequality

For arbitrary orientated analyzers, the degree of correlation between the results of the measurements on the two photons can be quantified by the quantity

$$E(\alpha, \beta) = P(V_\alpha, V_\beta) + P(H_\alpha, H_\beta) - P(V_\alpha, H_\beta) - P(H_\alpha, V_\beta) \, . \tag{1.5}$$

From this quantity, we can define the **Bell parameter** :

$$S(\alpha, \alpha', \beta, \beta') = E(\alpha, \beta) - E(\alpha, \beta') + E(\alpha', \beta) + E(\alpha', \beta') \, . \tag{1.6}$$

It is that parameter that allows one to distinguish between the hidden variable theory and the quantum theory. Indeed, Bell showed that according to the hidden variable theory, S should be lower than 2 no matter the state of the two photons. It is the so-called **Bell inequality**. On the other hand, the quantum theory predicts a value of S strictly greater than 2 for a Bell state, for a certain choice of angles of analysis.

P8 Show that $S = 2\sqrt{2}$ for the set of angles of analysis depicted in figure 1.2. In this configuration, the Bell inequality are maximally violated by quantum mechanics.

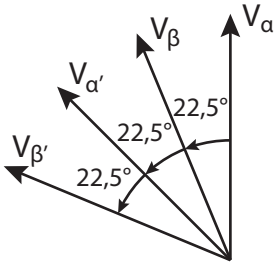

Figure 1.2: This set of angles of analysis maximizes the Bell parameter predicted by quantum mechanic.

3 Experimental implementation

3.1 Description of the experiment

The source of polarization-entangled photons consists in a laser diode emitting a $405\,\mathrm{nm}$ beam, vertically polarized and focused on two non-linear crystals of BBO. In those crystals, a parametric conversion process turn the $405\,\mathrm{nm}$ photons into a pair of $810\,\mathrm{nm}$ photons. One of the crystal generates pairs of photons with a vertical polarization, and the other one generates a horizontally-polarized pair. The twin photons are emitted symmetrically with respect to the probe beam, inside a cone with an aperture of about $3°$. An half-wave plate working at $405\,\mathrm{nm}$ and a Babinet compensator allows one to adjust the polarization state of the probe beam.

To collect the infrared photons, we use an avalanche photodiode (APD) on both side of the emission cone. Before entering into the detector, the infrared photons go through a polarization analyzer made of an half-wave plate, a polarization beam splitter (PBS), a lens to focus the beam onto the photodiode, and a interferential filter centered on $810\,\mathrm{nm}$ with a $10\,\mathrm{nm}$ width. A FPGA card is used to count the number of photons detected, as well as the number of coincidences, which correspond to a simultaneous detection on both arms. Those measurement are then displayed by a Labview code.

3.2 Single photons detection device

The detection devices are made of silicon APD used in single photon detection mode. On each arm A and B, the detection of a photon produce a TTL pulse ($0\,\mathrm{V}$ to $5\,\mathrm{V}$) with a temporal width of $25\,\mathrm{ns}$.

Warning ! Those detectors are very, very expensive and would be destroyed by a strong photon flux! Always check that the black tubes and the filters are installed to protect the photodiodes. Wait for the teacher authorization to switch on the detectors, and make sure that the main lights are off and the door is closed.

3.3 Events and coincidences counters

The FPGA card counts the TTL pulses emitted by the detectors (after a conversion from $0\,\mathrm{V}$ to $5\,\mathrm{V}$ to $0\,\mathrm{V}$ to $3{,}3\,\mathrm{V}$), and the number of coincidences between the A and B pulses within an adjustable integration time. To count the coincidences, the FPGA card proceeds as follows: when a pulse arrives on channel A, a time window of adjustable duration is open; if a pulse arrives on channel B before this window is closed, a coincidence is counted. The card send the counting information to the computer via a RS232 link, and the information is displayed by a Labview code. All the connections are already done, and we payed attention to the fact that the cables linking the APD to the coincidence counters have the same length.

Q1 Why do the cables need to have the same length?

$\rightsquigarrow$ Make the following settings:

- Before doing anything else, switch on the FPGA card, then start the Labview program and:
- Switch off every lights and turn the photons counters on.
- Measure the number of dark counts. The lower this number is, the better the detectors are.
- Switch a weak light and check that the number of detected photons stays well below $10^6\,\mathrm{photons/s}$.

3.4 Number of accidental coincidences.

For now, since the light sources are chaotic, the photons arriving in A and B are not correlated, and therefore the potential coincidences that you might detect are accidental. We note n_A and n_B the **counting rate** (average number of photons per second) on channels A and B, n_f the rate of accidental coincidences, and τ, the duration of the coincidence window.

Q2 Show that the rate of accidental coincidence is given by : $n_\mathrm{f} = n_A\, n_B\, \tau$.

The last two switches of the FPGA card, SW16 and SW17, allows one to choose the duration of the coincidence window (see table 3.1). The number given by this table are approximative and need to be re-measured.

SW16	SW17	τ (ns)
off	off	~ 70
on	off	~ 20
off	on	~ 14
on	on	~ 7

Table 1.1: Duration of the coincidence window.

$\rightsquigarrow$ Measure the rate of accidental coincidences for each of the four configurations.

Q3 Calculate the durations of the four coincidence windows using the formula established in question **Q2**.

This measure allows one to check the behavior of the coincidence counters. Call the teacher if the results are way different from the value of table 3.1.

3.5 Pump diode

The pump diode is a $405\,\mathrm{nm}$ laser with about $60\,\mathrm{mW}$ of output power. The light emitted by the diode is linearly polarized. The wearing of security glasses is mandatory!

$\rightsquigarrow$ Make the following settings:

- Press the two buttons to turn on the temperature regulator of the diode. The temperature is already set to obtain the correct wavelength. Don't try to change it.
- Press the two buttons to turn on the current supply of the diode, and set the current at maximum (about $95\,\mathrm{mA}$).
- If they are present on the bench, remove the optical elements mounted before the BBO crystals (half-wave plates at $405\,\mathrm{nm}$ and Babinet compensator) as well as the half-wave plates at $810\,\mathrm{nm}$ and the PBS cubes in front of the detection channels.
- Check the alignement of the beams (they should be already well aligned).

3.6 Parametric conversion

The photon pairs are produced by parametric down conversion in non-linear crystals β-BaB_2O_4 (baryum β-borate, BBO for short). During the non-linear process, a photon of the $405\,\mathrm{nm}$ pump can be converted in a pair of twin $810\,\mathrm{nm}$ photons. The BBO is a negative uniaxial birefringent crystal. We use a type I phase matching, meaning that the twin photons have the same polarization.

The pump beam is orthogonal to the entrance plane of the crystals. The optical axis of the crystals makes an angle of about $29°$ with the pump beam. The optical axis of the first crystal and the axis of the pump are forming a vertical plane, and the $810\,\mathrm{nm}$ twin photons emitted from this crystal are horizontally polarized (see figure 3.3). The optical axis of the second crystal and the axis of the pump are forming a horizontal plane, and the twin photons are emitted with a vertical polarization. In both cases, the twin photons are emitted symmetrically with respect to the pump axis, within a cone of about $3°$ of aperture.

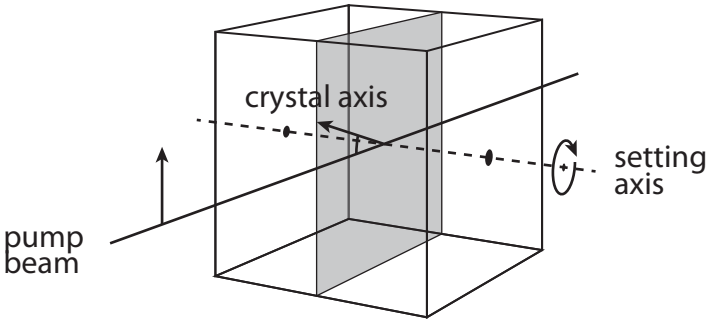

Figure 1.3: The optical axis of the crystal is oriented "vertically" with respect to the pump axis. The other crystal is oriented "horizontally".

Note: The direction of emission of the twin photons varies very quickly with the angle between the crystal axis and the pump axis. To optimize the number of twin photons arriving onto the detectors, one should carefully set the orientation of the two crystals, using the horizontal and vertical screws of the mount (see figure 3.3).

3.7 Settings of the collimation lens

To efficiently detect the pairs, the waist of the pump beam (which is inside the BBO crystals) is imaged onto the APD's sensitive surface. It is a difficult setting because this surface has a diameter of $180\,\mu\mathrm{m}$ only. The lenses have a focal

length of $75\,\mathrm{mm}$ and a diameter of $12{,}7\,\mathrm{mm}$. They are mounted $1040\,\mathrm{mm}$ away from the crystal.

Q4 Calculate the position of the image of the waist.

$\rightsquigarrow$ Check that the APD are approximatively at this position.

Q5 What is the magnification? Give an estimation of the diameter of the waist, then check that the size of the sensitive area of the photodiode is not limitating.

3.8 Optimization of the coincidence number

The direction of emission of the twin photons is very sensitive to the orientation of the crystals, which needs to be carefully optimized. The pump beam being vertically polarized, only the crystal whose axis is in a vertical plane can satisfy the phase matching condition for now. Its orientation can be adjusted thanks to the horizontal screw.

$\rightsquigarrow$ Optimize the number of coincidences by tuning the screw.

Q6 Calculate the number of accidental coincidences. Do we need to take it into account?

Q7 Calculate the ratio between the number of coincidences and the number of photons detected on each channel. Comment.

$\rightsquigarrow$ We will now optimize the orientation of the crystal whose axis is in an horizontal plane :

- Put the $405\,\mathrm{nm}$ half-wave plate before the BBO crystals.
- **Carefully identify the own axis of the plate (they do not correspond exactly to the 0 and $90°$ position). A good identification is crucial for the following**.
- Check that the number of coincidences is unchanged if the axis of the plate are horizontal and vertical. Explain why.
- Turn the plate at $45°$ to align the polarization of the pump beam with the horizontal axis.
- Optimize the number of coincidences by touching the vertical screw of the crystals.

3.9 $810\,\mathrm{nm}$ polarization analyzer

$\rightsquigarrow$ Put the $810\,\mathrm{nm}$ half-wave plates and the PBS cubes on each channel. Together they form a polarization analyzer (see figure 1.4).

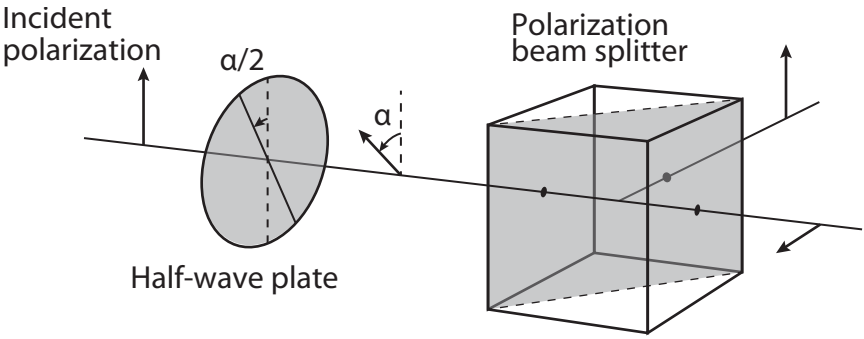

Figure 1.4: The polarization analyzer is made of an half-wave plate (whose orientation is adjustable) and a PBS cube.

Warning : The angle of the analyser is equal to the angle of analysis divided by two. So be careful to distinguish the angle of analysis from the angle of the plate!

Q8 Show that when the plate is vertical, the analyzer transmits the horizontal polarization, and therefore allows to detect the $|H\rangle$ photons. How much do you need to turn the plate to detect $|V\rangle$ photons?

$\rightsquigarrow$ Settings and adjustments:

- Check experimentally that the twin photons are in the state $|H\rangle_1 |H\rangle_2$ if the $405\,\mathrm{nm}$ half wave plate is vertical, and in the state $|V\rangle_1 |V\rangle_2$ if the plate is rotated by $45°$.
- If necessary, turn again the screws of the BBO crystals to have approximatively the same number of coincidences for those two positions of the plate.
- Then set the plate to $22{,}5°$ (try to be very precise) to obtain approximatively the same number of coincidences with the two analyzers in vertical position and the two analyzers in horizontal position (it is impossible to obtain a perfect equality, but try to balance the coincidences as much as you can).

$\rightsquigarrow$ Measure the number of coincidences when the two analyzers are parallel (horizontally or vertically). Measure the number of coincidences when the two analyzers are orthogonal.

$\rightsquigarrow$ Adjust the angle of the half-wave plate to obtain the same rate of coincidence in both situations.

$\rightsquigarrow$ Measure the coincidence rates when the two analyzers are parallel and perpendicular in the diagonal base (at $45°$).

$\rightsquigarrow$ Note the absolutely astonishing result of this measurement!

Q9 What results were you expecting? Compare with the previous measurement.

The previous settings produced a source of photon pairs created in either crystal equiprobably. This is a pair of entangled photons! Now you need to precisely adjust the polarisation state of the pump beam to obtain a Bell state.

3.10 Realization of a Bell state

For now, your twin photons are in the state

$$|\psi\rangle = \frac{1}{\sqrt{2}}\left(|V,V\rangle + e^{i\phi}|H,H\rangle\right) . \tag{1.7}$$

Where ϕ is the phase difference between the twin photons horizontally polarized, and the twin photons vertically polarized. This phase difference is linked to the birefringence of the BBO crystals.

Q10 Calculate the join probability $P(V,V)$ and $P(H,H)$ for the state (1.7). Does it allows you to distinguish the state (1.7) from the Bell state (1.2)?

Q11 Show that $P(V_{45°}, V_{45°}) = (1+\cos(\phi))/4$. What is the difference with the Bell state?

To obtain a Bell state instead of the state (1.7), you need to compensate the dephasing ϕ, by using a Babinet compensator. If the axis of the compensator match the horizontal and the vertical direction, you can translate it orthogonally to the pump axis to linearly vary the dephasing between the two polarisation components (see figure 1.5). For the pump wavelength, this dephasing typically varies by 2π for a translation of about $5\,\mathrm{mm}$.

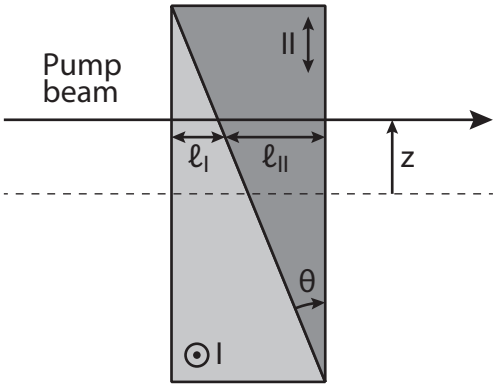

Figure 1.5: The Babinet compensator consist in two pieces of uniaxial birefringent crystal. The pieces are beveled and mounted one against the other, in such a way that the optical axis of the two crystals are orthogonal (and both parallel to the entrance plane). If we note n_1 the refractive index along the optical axis, and n_2 the refractive index along the direction orthogonal to the optical axis, we see that the dephasing $\phi_{\text{B}} = \phi_H - \phi_V$ accumulated between the polarisation components of a beam with a wavelength λ is given by $\lambda\phi_{\text{B}}/2\pi = (n_2\ell_{\text{I}} + n_1\ell_{\text{II}}) - (n_1\ell_{\text{I}} + n_2\ell_{\text{II}}) = 2(n_2 - n_1)\tan(\theta)\, z$.

$\rightsquigarrow$ Mount the compensator on the bench.

$\rightsquigarrow$ Check that the coincidence rate are still equal when the analyzers are parallel horizontally and vertically. If it is not the case, it means that the axis of the compensator do not match the vertical and horizontal directions, and you need to slightly rotate the compensator.

$\rightsquigarrow$ Put the analyzers at $45°$ on both channels and plot the coincidence rate as a function of the compensator translation over $10\,\text{mm}$ (by step of $0{,}5\,\text{mm}$). Take an integration time of $10\,\text{s}$.

Q12 Does the curve behave as expected? Comment on the contrast.

Q13 What are the points of the curve corresponding to a compensation of the dephasing induced by the crystals?

3.11 Variation of the join probability

The two theories we want to test (quantum theory and local hidden variable theory) do not predict the same variation of the join probability $P(V_\alpha, V_\beta)$ as a function of the relative angle $\alpha - \beta$. So it is interesting to measure it. Experimentally, we can estimate the probability $P(V_\alpha, V_\beta)$ by setting the analyzers at α and β and calculating the ratio between the coincidence rate and the photon rate on each channel.

Important note: Only complete the measurement below if you have enough time left before the end of the session. Otherwise, go directly to the Bell parameter measurement.

$\rightsquigarrow$ Fix the angle of one of the two analyzers at $0°$ and plot the variation of the coincidence rate as a function of the angle of the second analyzer. During this measurement, check that the photon rate on each channel remains approximatively constant. Re-do the same measurement, but this time set the first angle to $45°$.

Q14 Compare those measurements to the prediction of quantum mechanics (question **P6**).

3.12 Measure of the Bell parameter

You will now experimentally evaluate the Bell parameter defined by the relation (1.6), and whose value allows you to invalidate the local hidden variable theory. To do so, you will measure the join probabilities $P(V_\alpha, V_\beta)$, $P(H_\alpha, H_\beta)$, $P(V_\alpha, H_\beta)$ and $P(H_\alpha, V_\beta)$ for the following set of angles of analysis: $\{\alpha, \beta\}$, $\{\alpha, \beta'\}$, $\{\alpha', \beta\}$ and $\{\alpha', \beta'\}$ define on figure 1.2. To minimize the uncertainty of each measurement, one need to maximize the number of coincidences detected, so one needs to count them over a longer duration. Indeed, the fluctuations in the number of coincidences N_c detected over an interval T are linked to the photonic "shot noise", which has a Poisson statistics. This implies that the statistical uncertainty (standard deviation) $\sigma[n_\mathrm{c}]$ on the coincidence rate $n_\mathrm{c} = \langle N_\mathrm{c} \rangle / T$ verifies :

$$\sigma[n_\mathrm{c}] = \frac{\sigma(N_\mathrm{c})}{T} = \frac{\sqrt{\langle N_\mathrm{c} \rangle}}{T} = \sqrt{\frac{n_\mathrm{c}}{T}}\,, \tag{1.8}$$

so that the relative uncertainty

$$\frac{\sigma[n_\mathrm{c}]}{n_\mathrm{c}} = \frac{1}{\sqrt{\langle N_\mathrm{c} \rangle}} = \frac{1}{\sqrt{n_\mathrm{c} T}}\,. \tag{1.9}$$

Q15 If you count an average of $100\,\mathrm{coincidences/s}$, what is the standard deviation of the coincidence rate? What is the duration required to divide this standard deviation by 10?

$\rightsquigarrow$ Fill the Excel chart on the computer for each of the 16 measurements. Take an integration time of 10 or $20\,\mathrm{s}$ to have a good precision. The Bell parameter is then automatically calculated.

Q16 What value of the Bell parameter do you obtain and what are the error bars? Does your measurement allow you to invalidate the local hidden variable theory or the quantum theory?

Q17 What result would allow you to invalidate quantum mechanics?

P 2

Saturated absorption Sub-Doppler spectroscopy

Contents

At room temperature, the main cause of the broadening of atomic transitions in a gas is the Doppler effect. Saturated absorption spectroscopy, developed in the 1970s, makes it possible to overcome this broadening and resolve the hyperfine structure of atomic transitions. The aim of the practical work is to carry out saturated absorption spectroscopy of the D1 line of rubidium in order to observe its hyperfine structure. The source used is a laser diode tunable in wavelength around 795 nm.

1 Preliminary study

1.1 Doppler broadening

We consider an atomic gas of two-level atoms and denote ν_0 the frequency of the atomic transition. Doppler broadening, which is largely predominant at room temperature, results from the dispersion of the velocities of the atoms in the gas. The gas is illuminated by a laser beam of frequency ν propagating along the axis Oz in the positive direction. Among the atoms, only those whose V_z projection of the velocity along Oz satisfies the relation

$$\nu_0 = \nu\,(1 - V_z/c) \tag{2.1}$$

are in resonance with the wave and can absorb and re-emit light (c is the speed of light). Thus, if we sweep the laser frequency, **we obtain an absorption line profile that reflects the distribution of atomic velocities in the direction of the laser beam**.

P1 Quickly explain the demonstration of the formula (2.1).

Statistical physics shows that the velocity distribution of atoms in a perfect gas follows the Maxwell-Boltzmann law:

$$f(V_z) = \left(\frac{m}{2\pi \mathrm{k_B} T}\right)^{1/2} \exp\left(\frac{-mV_z^2}{2\mathrm{k_B}T}\right). \tag{2.2}$$

In this equation, V_z is the velocity along the z axis, T is the temperature of the gas, m is the mass of the atoms ($1.41\ 10^{-25}\,\mathrm{kg}$ for rubidium) and $\mathrm{k_B}$ is Boltzmann's constant ($1.38\ 10^{-23}\,\mathrm{J/K}$).

P2 Show that the width at half-height of the line broadened by the Doppler effect is :

$$\Delta\nu = \sqrt{8\ln 2}\sqrt{\frac{\mathrm{k_B}T}{m}}\frac{\nu_0}{c}\ . \tag{2.3}$$

P3 Use the formula 2.3 to calculate the Doppler broadening at $T = 20^\circ$ of the rubidium D1 line (centred at $795\,\mathrm{nm}$).

1.2 Structure of the rubidium D1 line

The rubidium cell you are going to use contains the two stable isotopes of the atomic species in the proportions of their natural abundance: 72% rubidium 85 and 28% rubidium 87. The wavelength of study ($795\,\mathrm{nm}$) corresponds to the transition from the fundamental level $5\mathrm{S}_{1/2}$ to the excited level $5\mathrm{P}_{1/2}$. The hyperfine structure is detailed in figure 2.1 for both isotopes.

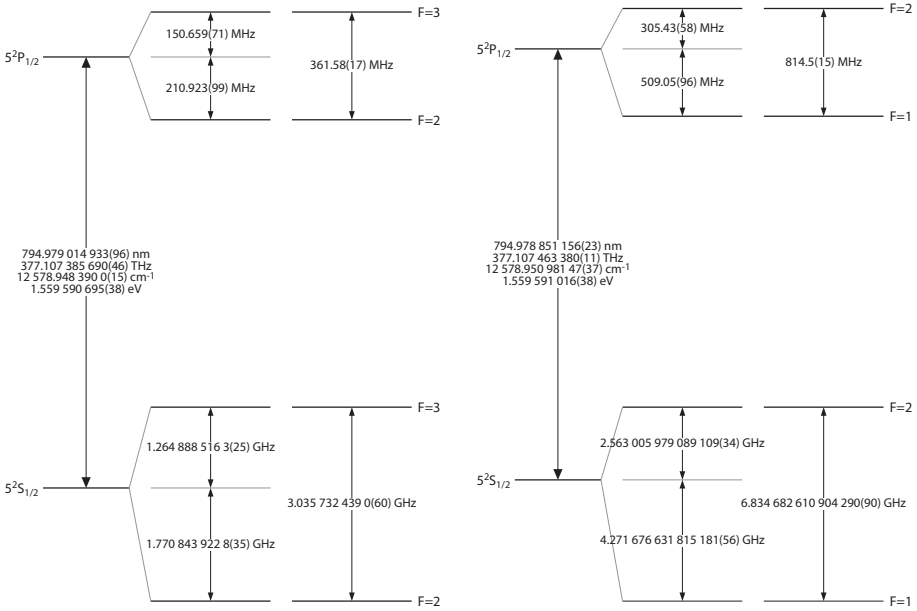

(a) Rubidium 85 **(b)** Rubidium 87

Figure 2.1: Hyperfine structure of the D1 line of the two rubidium isotopes. The figure is taken from: Daniel A. Steck, *Rubidium D Line Data*, available online at `http://steck.us/alkalidata`.

P4 How many lines should we theoretically observe? Arrange these lines in ascending order of resonance frequency.

P5 Taking Doppler broadening into account, which lines can be resolved with a simple absorption spectrum? At what temperature would we need to go down to resolve the entire hyperfine structure? Knowing that the natural width of the excited levels is $6\,\mathrm{MHz}$, at what temperature would we have to go down to be able to measure it? How can this be achieved?

1.3 Saturation of absorption

Let's now return to a two-level gas of atoms. In general terms, the absorption $\mathcal{A}$ (in cm^{-1}) of a laser beam of frequency equal to the atomic transition frequency is given by the effective resonance scattering cross-section σ_0 (in cm^2) weighted by the difference between the densities of atoms in the fundamental level, n_1, and in the excited level, n_2 (in cm^{-3}). This difference in density depends on the

intensity I (in $\mathrm{W.cm^{-2}}$) of the laser beam and therefore on the absorption $\mathcal{A}$. This process of circular dependence ($\mathcal{A}$ depends on $n_1 - n_2$, which depends on I, which depends on $\mathcal{A}$) gives rise to the phenomenon of absorption saturation. In concrete terms, we show that:

$$\mathcal{A} = \sigma_0 \times (n_1 - n_2) \quad \text{avec} \quad n_1 - n_2 = \frac{n_\mathrm{t}}{1 + I/I_\mathrm{sat}} \,, \tag{2.4}$$

where n_t is the total density of atoms and I_sat is an intensity characteristic of the transition, called the **saturation intensity**, which is $1.6\,\mathrm{mW/cm^2}$ for the atomic transition under consideration. The ratio $s = I/I_\mathrm{sat}$, which is used in the equation 2.4, is called the **saturation parameter**.

P6 Make a qualitative comparison of the absorption in the limiting cases $s = I/I_\mathrm{sat} \ll 1$ and $s = I/I_\mathrm{sat} \gg 1$. What about absorption in the case of high intensity ($s \gg 1$). **This phenomenon is called absorption saturation**.

P7 Give the limit of the populations n_1 and n_2 in the case of strong saturation. Give an interpretation of absorption saturation by considering the evolution of the spontaneous emission rate as a function of intensity.

P8 Is it possible to invert the populations on a 2-level system? Explain why.

1.4 Application to sub-Doppler spectroscopy (pump-probe method)

Consider two laser beams of the same frequency ν and counter-propagating (superimposed but propagating in opposite directions). The first beam, called the pump beam, propagates in the positive direction of the Oz axis and has sufficient intensity to saturate the absorption on the transition in question. The second beam, called the probe beam, propagates in the negative direction of the Oz axis and has too low an intensity to saturate the transition on its own. We are interested here in the absorption of the probe beam in the presence of the pump beam when their frequency is varied around the frequency of the atomic transition.

According to equation 2.1, for a given frequency ν, the atoms which absorb the pump are those for which $V_z = -c\,(1 - \nu/\nu_0)$ and the atoms which absorb the probe are those for which $V_z = +c\,(1 - \nu/\nu_0)$. There are then two cases, represented in figure 2.2 :

- if $\nu \neq \nu_0$, the atoms which absorb the pump and those which absorb the probe belong to different velocity classes. In this case, the presence of the pump has no effect on the absorption of the probe;

- if $\nu = \nu_0$, the same atoms absorb the pump and the probe, i.e. atoms with zero velocity along z ($V_z = 0$). As the pump is sufficiently intense to saturate the absorption, the probe is absorbed very little (absportion is reduced) at this precise frequency $\nu = \nu_0$.

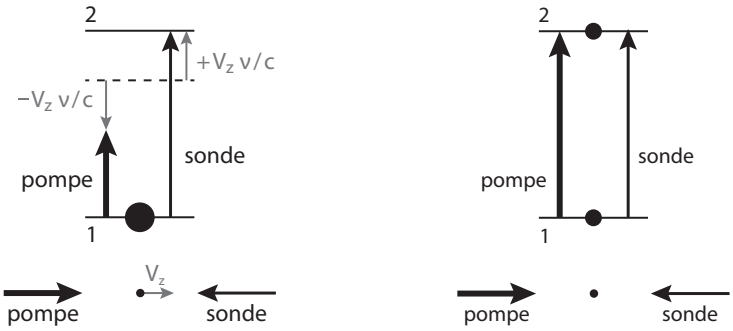

(a) $\nu < \nu_0$ **(b)** $\nu = \nu_0$

Figure 2.2: Influence of the Doppler effect in the pump-probe configuration.

The absorption line profile of the probe therefore has a dual structure, with a narrow peak centred on the frequency of the atomic transition superimposed on the profile broadened by the Doppler effect. As you will see in the course of the labwork, the resolution offered by pump-probe spectroscopy is such that it can reveal the hyperfine structure of the atomic transition. Each transition then appears as a distinct peak in the Doppler profile, as shown in Figure 2.3.

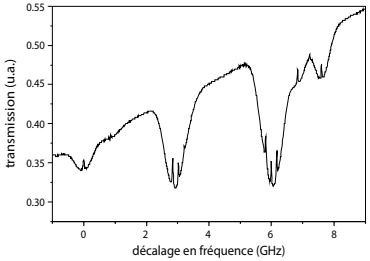

Figure 2.3: Absorption spectrum around $795\,\mathrm{nm}$ obtained by the pump-probe method. The lines of the hyperfine structure appear as narrow peaks against a background broadened by the Doppler effect. The figure is adapted from: Svenja A. Knappe *et al.*, *Microfabricated saturated absorption laser spectrometer*, Optics Express **15**, 6293–6299 (2007).

P9 What is the intrinsic width of the saturated absorption peak? What are the reasons why this peak might appear wider?

2 Experimental realization

Precautions for using the laser diode Never disconnect the cables connecting the laser diode to its power supply. **The maximum power delivered by the diode is of the order of 30 to 50 mW, which is enough to cause irreversible eye damage in direct vision**. As the eye is not very sensitive to this wavelength, the beam can reach you without you noticing. So be careful not to put your eyes at bench level. Remove or hide any reflective objects that may be at beam level (watches, bracelets, rings, chains, bracelets, belt buckles, etc.). Check that all optical elements are firmly attached to the board when the diode is transmitting. Finally, use the laser safety glasses provided at the entrance to the room.

General precautions All the optical elements used are fragile, expensive and difficult to obtain (particularly the cell containing the rubidium). You will be making difficult adjustments, in the dark, and with a near-infrared viewfinder (which is not very convenient). So move the elements carefully, clamp the feet carefully after each modification and don't leave anything lying around the edge of the board.

2.1 Laser diode

The tunable laser used here is a "DBR" (Distributed Bragg Reflector) laser diode, which provides single-mode operation at a very fine instantaneous laser linewidth (around MHz, i.e. around 2 $10^{-6}\,\mathrm{nm}$!!). However, fluctuations in current and temperature will introduce fluctuations in this frequency and cause it to broaden. In practice, the actual frequency linewidth is therefore higher, of the order of a few tens of MHz.

The laser diode package includes an optical fiber to prevent perturbing backward light reflection into the cavity [1], and the light is directly injected into a single mode polarizing maintaining optical fiber.

The laser emission frequency is a function of two parameters: the equilibrium temperature T_{eq} of the junction and the intensity i of the diode injection

[1] Laser diodes are very sensitive to reflections (even very weak ones) from the beam towards the cavity, which can introduce significant fluctuations in the emission length. It is therefore necessary to use an optical isolator. This blocks the reverse return of light by using a Faraday rotator placed between two polarisers. The Faraday rotator used rotates a 45° rectilinear polarisation in the same direction regardless of the direction in which the light travels, so that if the polarisers are oriented to allow light propagating in one direction to pass, they will necessarily block light propagating in the other direction.

current. The emission frequency increases with T_{eq} and decreases with i (the wavelength increases with the current). In this labwork, we will vary the emission frequency using the current alone. The full characteristics of the laser diode used are detailed in the document at your disposal.

Temperature controller The junction equilibrium temperature is measured by a thermistor. The set temperature is fixed by a resistance value. Its value is preset so that the entire spectrum around line D1 can be observed by sweeping the current alone. **In principle, you will not need to change this setting**. If, however, you need to change the set temperature, to move away from a mode jump for example, be careful to do so only in very small steps. A sudden change would take you too far away from resonance and it would be difficult to find it again afterwards.

Current supply By default, set the current to around $120\,\text{mA}$ so that you can view the beam using the infra-red card (or simply on a piece of paper).

P10 If you want to see all the transitions in the rubidium D1 line for both isotopes, over what range should you vary the current in the laser diode?

P11 Compare the spectral width of the laser with the natural width of the atomic transition. Which of these two widths will determine the width of the absorption lines observed once the Doppler effect has been eliminated?

2.2 Fluorescence and absorption spectra

$\rightsquigarrow$ Place the cell in the path of the laser beam and adjust the observation camera so that the inside of the cell is clearly visible.

$\rightsquigarrow$ In total darkness, slowly vary the value of the current. In this way, you should be able to observe the fluorescence of the rubidium in the D1 line using the camera: the path of the laser beam shines in the cell for a precise value of current!

$\rightsquigarrow$ Once you have obtained fluorescence, complete the set-up described in figure 2.4. To visualise the lines of the two isotopes contained in the cell, sweep the diode's emission frequency by modulating the driving current with a triangular signal.

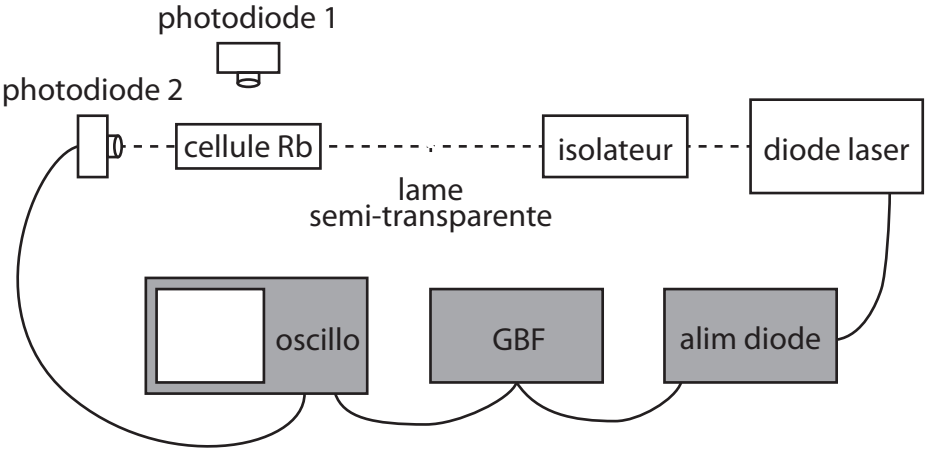

Figure 2.4: Schéma du montage à réaliser pour observer les spectres de fluorescence et d'absorption.

⇝ Switch on the GBF and set it to produce a low-amplitude triangular signal at a frequency of around 10 Hz. Display the GBF signal on one of the oscilloscope channels.

⇝ Place one of the two photodiodes carefully against the cell (without contact), perpendicular to the laser beam, to capture part of the fluorescence signal. Monitor the photodiode signal on the other channel of the oscilloscope (set the adjustable gain to maximum) .

⇝ Modify the amplitude of the modulation applied to see the different fluorescence lines expected. Improve the signal obtained (by averaging if necessary.

⇝ Save the displayed signals with an USB stick (or take a photo of the screen, after you've turned on "stop").

Q1 Identify the different lines on the oscillogram and briefly explain how you did this.

Q2 Calibrate the oscillogram using the largest gap between two lines as a reference. Measure and check the spacing and relative positions of the different lines. Check that the width of the lines corresponds to that expected from the Doppler effect (or at least is of the right order of magnitude).

$\rightsquigarrow$ Place the second photodiode behind the cell and display the absorption spectrum on the oscilloscope channel previously occupied by the GBF (the GBF is moved to the synchro input). **Caution: adjust the gain to make sure you don't saturate the signal coming out of the photodiode, which happens very quickly!**.

$\rightsquigarrow$ Observe the fluorescence and absorption spectra simultaneously.

$\rightsquigarrow$ Observe the changes in the absorption spectrum when a density is added before the cell.

$\rightsquigarrow$ Now observe what happens if you place the density after the cell, and compare it with the previous situation (density before the cell).

$\rightsquigarrow$ Using the power meter provided, **measure the values of the saturation parameter** $s = I/I_{\mathbf{sat}}$ for the intensity incident on the cell (with or without density).

Q3 Explain why the phenomenon of absorption saturation is clearly demonstrated qualitatively.

2.3 Sub-Doppler spectroscopy of hyperfine levels

The pump-probe setup is shown in Figure 2.5. The pump and probe beams must be superimposed at the gas cell.

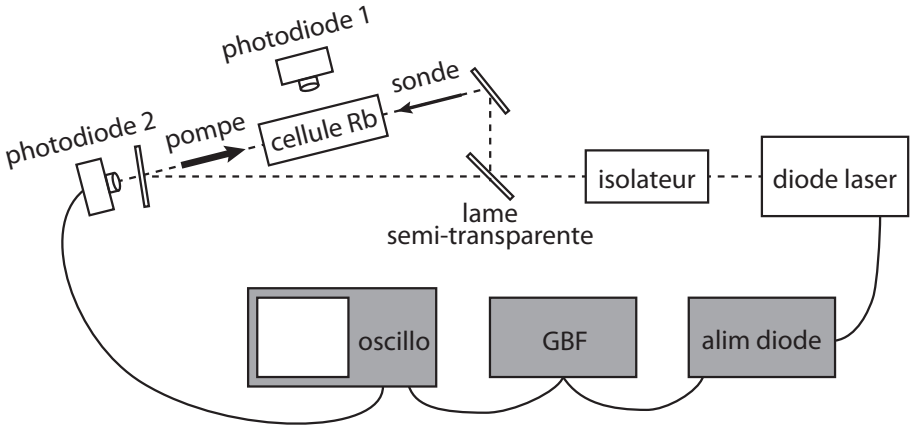

Figure 2.5: Schéma du montage en configuration pompe-sonde.

$\rightsquigarrow$ Do not touch the power supply or GBF settings!

$\rightsquigarrow$ First place and adjust all the components, excluding the cell and photodiodes. Carefully superimpose the pump and probe beams, observing the laser spots on on separating plates with the infrared viewer.

$\rightsquigarrow$ Using the power meter, measure the values of the saturation parameter $s = I/I_{\text{sat}}$ for the pump and probe in this configuration.

$\rightsquigarrow$ Then position the cell and the photodiodes to visualise absorption on the probe beam and the fluorescence.

$\rightsquigarrow$ Save the displayed signals with an USB stick (or take a photo of the screen, after you've turned on "stop").

Q4 For the two isotopes, identify the lines of the hyperfine structure (using figure 2.1). Measure the relative positions of the hyperfine lines and compare the values obtained with the expected values. Also measure the width of the observed lines.

Q5 What do they correspond to?

In Doppler profiles covering two atomic transitions (as for rubidium 85), instead of 2 absorption lines you should observe 3 lines. The third line appears precisely in the middle of the 2 expected lines. This phenomenon is called crossover.

Q6 Explain the origin of the crossover line. To do this, repeat the reasoning given in section **??** for the case of an atom with two excited states.

Q7 Compare the absorption and fluorescence spectra. Is it possible to see the same saturation signature in the fluorescence spectra? Explain why.

P 3

Hong, Ou and Mandel experiment

1 Introduction

The Hong, Ou and Mandel (HOM) experiment, conducted in 1987 [1], is the first observation of a quantum interference between two photons with no classical explanation (*i.e.* no explanation with a wave description of light). This phenomenon appears when two indistinguishable photons arrive simultaneously at the two input ports of a 50/50 beam splitter. The distribution of the two photons between the two output ports of the beam splitter exhibit a surprising behavior, that can not be explained with a classical theory of light...

1.1 The HOM effect

If a photon arrives on a 50/50 beam splitter, it has 1/2 probability of being transmitted or reflected. When two photons arrive simultaneously on a beam splitter, each one at a different input (a or b), there are four possibilities (see figure 3.1) :

- The photon entered in a goes out in c, and the photon entered in b goes out in d;
- The photon entered in a goes out in d, and the photon entered in b goes out in c;
- Both photons go out in c ;

[1] C. K. Hong, Z. Y. Ou et L. Mandel, *Measurement of subpicosecond time intervals between two photons by interference*, Physical Review Letters **59**, 2044 (1987)

- Both photons go out in d.

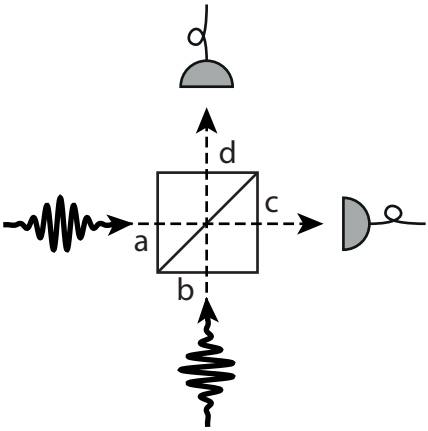

Figure 3.1: Two indistiguishable photons arrive simultaneously on a beam splitter. Two single-photon detectors at the output c and d record which way the photons went out.

If the photons were classical particles, the 4 cases would always be equiprobable, in the case where the reflectivity and transmitivity of the beam splitter are equal. But according to the quantum theory, if the two particles are **indistinguishable** there is no way to know which particle is which at the output of the beam splitter, and therefore there is only 3 possible **observations** :

- we observe one photon in each output ;
- we observe two photons in output c ;
- we observe two photons in output d.

Then, according to quantum mechanics, the probability of observing a photon in each output results from the **interference** between the two **classical trajectories** $(a, b) \to (c, d)$ and $(a, b) \to (d, c)$. It then depends on the **relative phase** associated to those trajectories.

In our case, two photons are **indistinguishable** when their properties (polarization, frequency, transverse mode) can not be distinguished with our experimental setup. Note that the two photons do not need to be identical, which would imply that they have identical properties, for them to be indistinguishable. For instance, two photons with different frequencies (or energies) behave as indistinguishable photons as long as the experimental setup does not allow one to measure the difference in their frequencies. As a consequence,

establishing whether two photons are indistinguishable or not depends on the experimental setup which is used.

1.2 Formalism

In classical electromagnetism, a beam splitter is modelled by a **real unitary matrix** , that links the **electrical fields** $\mathcal{E}_{a,b}$ of the inputs to the electrical fields $\mathcal{E}_{c,d}$ of the outputs:

$$\begin{pmatrix} \mathcal{E}_c \\ \mathcal{E}_d \end{pmatrix} = U \begin{pmatrix} \mathcal{E}_a \\ \mathcal{E}_b \end{pmatrix} \quad \text{with} \quad U = \begin{pmatrix} t & r \\ -r & t \end{pmatrix} . \tag{3.1}$$

The unitarity property $U^\dagger U = \mathbb{1}$ stands for the **energy conservation** between the input and the output of the beamsplitter. It leads to a relationship between the reflectivity and transmitivity coefficient of the beam splitter.

$$r^2 + t^2 = 1 . \tag{3.2}$$

A $50/50$ beam splitter corresponds to the case where $r = t = 1/\sqrt{2}$.

In quantum optics, the complex electromagnetic field is replaced by **creation and annihilation operators** :

$$\mathcal{E}_a \to \{\hat{a}, \hat{a}^\dagger\} , \ \mathcal{E}_b \to \{\hat{b}, \hat{b}^\dagger\} , \ \mathcal{E}_c \to \{\hat{c}, \hat{c}^\dagger\} , \ \mathcal{E}_d \to \{\hat{d}, \hat{d}^\dagger\} . \tag{3.3}$$

The beam splitter links those operators in the same way than with the electric fields :

$$\begin{pmatrix} \hat{c} \\ \hat{d} \end{pmatrix} = U \begin{pmatrix} \hat{a} \\ \hat{b} \end{pmatrix} \quad \text{and} \quad \begin{pmatrix} \hat{c}^\dagger \\ \hat{d}^\dagger \end{pmatrix} = U \begin{pmatrix} \hat{a}^\dagger \\ \hat{b}^\dagger \end{pmatrix} . \tag{3.4}$$

The unitarity property of the matrix U ensures that **the number of photons is conserved** between the input and the output :

$$\hat{c}^\dagger \hat{c} + \hat{d}^\dagger \hat{d} = \hat{a}^\dagger \hat{a} + \hat{b}^\dagger \hat{b} . \tag{3.5}$$

The quantum state that corresponds to a situation where two photons enter in a and b is obtained by using the operators $\hat{a}^\dagger$ and $\hat{b}^\dagger$ on the state which corresponds to the **electromagnetic vacuum** : $\hat{a}^\dagger \hat{b}^\dagger |\text{vacuum}\rangle$. By inverting the relation 3.4, one can link this input state to the output state:

$$\begin{aligned} \hat{a}^\dagger \hat{b}^\dagger |\text{vacuum}\rangle &= (t\hat{c}^\dagger - r\hat{d}^\dagger)(r\hat{c}^\dagger + t\hat{d}^\dagger)|\text{vacuum}\rangle \\ &= (tr\hat{c}^\dagger \hat{c}^\dagger + t^2 \hat{c}^\dagger \hat{d}^\dagger - r^2 \hat{d}^\dagger \hat{c}^\dagger - rt\hat{d}^\dagger \hat{d}^\dagger)|\text{vacuum}\rangle . \end{aligned} \tag{3.6}$$

In the case of a $50/50$ beam splitter, we can use the commutativity of the operators acting on the different modes of the electromagnetic field. The last expression then become:

$$\hat{a}^\dagger \hat{b}^\dagger |\text{vacuum}\rangle = \frac{1}{2}(\hat{c}^\dagger \hat{c}^\dagger - \hat{d}^\dagger \hat{d}^\dagger)|\text{vacuum}\rangle \ . \tag{3.7}$$

The interpretation of this equation is straightforward: at the output of the beam splitter, the states corresponding to the situation where two photons are at the output c or d are equiprobable, but the probability of having a photon on each output is zero. Therefore **we never observe any coincidence** between the detectors c and d.

2 Experimental realization

2.1 Description of the experimental setup

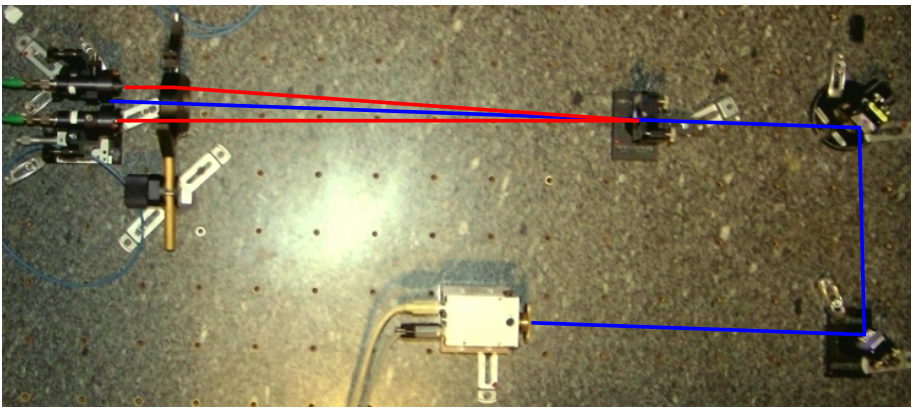

Figure 3.2: View from above. We see the laser diode, two mirrors to set the alignement, the non-linear crystal, the optics for the conjugation and two fibered collimators. The optical path of the pump beam and the photons pairs are sketched.

To observe the HOM effect, one needs to create pairs of indistinguishable photons and send them into a beam splitter (see figure 3.2). To do so, we will use a parametric down-conversion process inside a $\chi^{(2)}$ non-linear crystal (BBO) than can convert a pump photon at $\lambda_p = 405\,\text{nm}$ into a pair of photons at $2\lambda_p = 810\,\text{nm}$. The twin photons are emitted symmetrically with respect to the pump axis, within a cone of about 3° of aperture. The pump beam, emitted from a laser diode, is horizontally polarized. The twin photons created in this process, are vertically polarized.

The twin photons are then injected inside two polarization-maintaining monomode fibers, thanks to a pair of fibered collimators and an optical doublet, whose focal point is set inside the crystal. An interferometric filter at $810\,\mathrm{nm}$ allows us to get rid of most of the stray lights. The fibered light then enters inside a module made of two waveguides that will play the role of the beam splitter. The waveguides are mounted very close to each other so that the transverse mode of the light propagating in each waveguide overlap the other one. The fibers are connected to a detection module using Avalanche PhotoDiodes (APD). A FPGA card is used to count the number of detected photons in each output. A simultaneous detection on each output is counted as a **coincidence**. A Labview code is then used to display the number of events and coincidences.

2.2 Single photon detection module

The single photon detection module is an exceptional tool, adapted for this kind of experiment. It is made of four fibered channels, linked to four APDs. On each channel, the detection of a photon triggers the emission of a $25\,\mathrm{ns}$ TTL pulse ($0\,\mathrm{V}$ to $5\,\mathrm{V}$). We will just use two channels out of four for this experiment, labeled A and B.

Warning ! Those detectors are very, very expensive and would be destroyed by a strong photon flux! Always check that the interferometric filters are installed to protect the photodiodes. Wait for the teacher authorization to switch on the detectors, and make sure that the main lights are off and the door is closed.

2.3 Event and Coincidence counter

The FPGA card counts the TTL pulses emitted by the detectors (after a conversion from $0\,\mathrm{V}$ to $5\,\mathrm{V}$ to $0\,\mathrm{V}$ to $3{,}3\,\mathrm{V}$), and the number of coincidences between the A and B pulses within an adjustable integration time. To count the coincidences, the FPGA card proceeds as follows: when a pulse arrives on channel A, a time window of adjustable duration is open; if a pulse arrives on channel B before this window is closed, a coincidence is counted. The card send the counting information to the computer via a RS232 link, and the informations are displayed by a Labview code. All the connections are already done, and we payed attention to the fact that the cables linking the APD to the coincidence counters have the same length.

Q1 Why do the cables need to have the same length?

$\rightsquigarrow$ Perform the following settings and measurements:

- Before doing anything else, switch on the FPGA card, then start the Labview program.
- Switch off every lights and turn the photons counters on.
- Measure the number of dark counts. The lower this number, the better the detectors are.
- Switch on a distant light and check that the number of detected photons stays way below 10^6 photons/s.

2.4 Number of accidental coincidences.

For now, since the light sources are chaotic, the photons arriving in A and B are not correlated, and therefore the coincidences are accidental. We note n_A and n_B the **counting rate** (average number of photons per second) on channels A and B, n_f the rate of accidental coincidence, and τ, the duration of the coincidence window.

Q2 *Show that the rate of accidental coincidence is given by :* $n_f = n_A\, n_B\, \tau$.

The last two switches of the FPGA card, SW16 and SW17, allow one to choose the duration of the coincidence window (see table 3.1). The numbers given in this table are approximate and must need be measured.

SW16	SW17	τ (ns)
off	off	~ 70
on	off	~ 20
off	on	~ 14
on	on	~ 7

Table 3.1: Duration of the coincidence window.

$\rightsquigarrow$ Measure the rate of accidental coincidences for each of the four configurations and calculate the durations of the four coincidence windows using the formula established in question 2.

This measure allows one to check the behavior of the coincidence counters. Call the teacher if the results are different from the value of table 3.1.

2.5 Pump diode

The pump diode is a $405\,\mathrm{nm}$ laser with about $60\,\mathrm{mW}$ of output power. The light emitted by the diode is linearly polarized. The wearing of security glasses is mandatory!

$\rightsquigarrow$ Make the following settings:

- Press the two buttons to turn on the temperature regulator of the diode. The temperature is already set to obtain the correct wavelength. Don't try to change it.

- Press the two buttons to turn on the current supply of the diode, and set the current at maximum (about $95\,\mathrm{mA}$).

- Briefly check the alignement of the beams (they should be already well aligned).

2.6 Parametric conversion

The photons pairs are produced by parametric down conversion in non-linear crystals β-BaB2O4 (baryum β-borate, BBO for short). During the non-linear process, a photon of the $405\,\mathrm{nm}$ pump can be converted in a pair of twin $810\,\mathrm{nm}$ photons. Recall that the two photons of the pair may have slightly different energies (or wavelenghts) since only their sum is set by the energy of a $405\,\mathrm{nm}$ pump photon (energy conservation in the process of parametric down conversion).

The BBO is a negative uniaxial birefringent crystal. We use a type I phase matching, meaning that the twin photons have the same polarization.

Q3 Recall what are the two conditions satisfied by a non-linear process. Which one is called the phase matching condition?

The pump beam is orthogonal to the entrance plane of the crystal. The optical axis of the crystal and the axis of the pump are forming an horizontal plane (see figure 3.3).

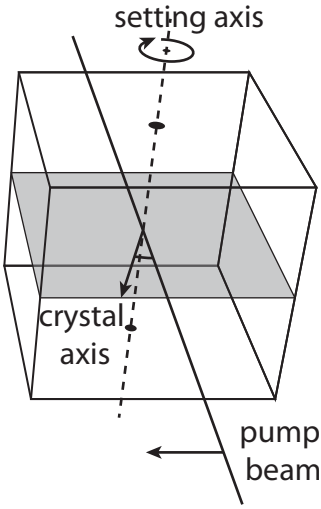

Figure 3.3: Orientation of the optical axis of the crystal with respect to the pump axis.

The pump is horizontally (extraordinary) polarized and the $810\,\mathrm{nm}$ twin photons emitted from the crystal are vertically (ordinary) polarized. The refractive indexes n_o and n_e which characterize respectively the crystal axis and the orthogonal axis are given in table 3.2. From those indexes, one can calculate the index n_θ seen by the pump while it propagates through the crystal:

$$1/n_\theta^2 = \sin^2(\theta)/n_o^2 + \cos^2(\theta)/n_e^2\,. \tag{3.8}$$

θ being the angle between the propagation axis and the crystal axis (see figure 3.3).

wavelength (nm)	n_o	n_e
405	1,691 835	1,567 071
810	1,660 100	1,544 019

Table 3.2: Refractive index of the BBO crystal along its optical axis, at a temperature of $293\,\mathrm{K}$.

Q4 Using a spreadsheet (Excel), calculate $n_\mathrm{e}(405, \theta)$ as a function of θ in the near range of $\theta = 30^\circ$. For what precise angle θ is type I collinear phase tuning achieved?

If we deviate slightly from this precise θ angle by modifying the crystal's inclination, we'll still obtain a type I, but non-collinear, phase tuning.

Q5 The collimators are positioned in such a way that they are forming with the crystal an isosceles triangle, with a 3° aperture. What should be the angle θ for the twin photons to be correctly collected by the collimators?

2.7 Settings of the collimators

The optical fibers are polarization-maintaining fibers. Their own axis are parallel to the horizontal and vertical axis. One of the own axis can be spotted thanks to a tip on the connector.

Q6 Why are those polarization-maintaining fibers crucial to observe the HOM effect?

Now you need to image the area of emission of the photons pairs onto the core of each fibers, by tuning the orientation of the collimators. This is a difficult setting because the fibers' cores have a diameter of $5\,\mu\mathrm{m}$ only. A trick is to make light propagates in the other direction (from the collimators to the crystal) by injecting a $670\,\mathrm{nm}$ auxiliary laser at the output of the polarization-maintaining fibers. You then have two beams coming out of the collimator. Focalise them inside the crystal and superimpose them to the pump beam. Of course you need to take the filter away from the collimator because they would cut the $670\,\mathrm{nm}$ light. Don not forget to put them back before switching the photon counters on again.

Warning ! You must switch the single photon detection module off every time the fibers are disconnected, and every time the filter are taken away from the collimators. Don not forget to put them back before switching the photon counters on again. Always protect the fibers' extremity with a cap.

Even with this method, it is difficult to inject the fibers. You will have to be very cautious (and probably try several times) to set the collimators correctly. However, as soon as you manage to inject a small fraction of the twin photons, the setting becomes a lot easier, you then just have to optimize the number of coincidences by fine-tuning the position of the collimators.

Remark The screws of the collimators' mounts are the only elements you need to touch during this setting. If you lose all the signal in the process (and you are not able to recover it) call the teacher.

$\rightsquigarrow$ Measure the coincidences rates.

Q7 Calculate the rate of accidental coincidences.

Q8 Do you need to account for them?

2.8 Observation of the HOM effect

Once the coincidence rate is high enough (about $600\,\mathrm{coincidences/s}$), you are ready to observe the HOM effect. One of the collimators is mounted on a translation stage. Record the number of coincidences as you gently move the translation stage (for instance by step of $10\,\mu\mathrm{m}$). To lower the uncertainty of your measurements, you need to raise the number of detected coincidences, so you need to count coincidences over a longer time interval. The fluctuations of the number of coincidences N_c measured during a time T is linked to the photonic shot noise, which follows a Poisson law. It means that the standard deviation $\sigma[n_\mathrm{c}]$ on the coincidence rate $n_\mathrm{c} = N_\mathrm{c}/T$ verifies :

$$\sigma[n_\mathrm{c}] = \frac{\sigma(N_\mathrm{c})}{T} = \frac{\sqrt{N_\mathrm{c}}}{T} = \sqrt{\frac{n_\mathrm{c}}{T}}\,., \tag{3.9}$$

which leads to the relative uncertainty :

$$\frac{\sigma[n_\mathrm{c}]}{n_\mathrm{c}} = \frac{1}{\sqrt{N_\mathrm{c}}} = \frac{1}{\sqrt{n_\mathrm{c}T}}\,. \tag{3.10}$$

Q9 Assuming you count an average of $100\,\mathrm{coincidences/s}$, what is the standard deviation on the coincidence rate? How long should the time interval be to reduce this deviation by a factor of 10?

In practice, you will count the coincidences during a time interval of 10 or $20\,\mathrm{s}$.

$\rightsquigarrow$ Plot the coincidence rate as a function of the position of the translation stage. Add the error bars on your graph.

Q10 Interpret the curve.

$\rightsquigarrow$ What is the depth of the dip?

Q11 Why does it not go to zero?

$\rightsquigarrow$ What is the the full width at half minimum of the dip?

Q12 Compair it to the coherence length of the $810\,\mathrm{nm}$ photons, which is given by the the filter ($10\,\mathrm{nm}$ width).

The width of the HOM dip is given by the energy difference of the twin photons created.

Q13 Explain why, using the notion of indistinguishability of the photons detected.

It is now possible to add interference filters of width $5\,\mathrm{nm}$.

Q14 What width of dip should we get in this case?

$\rightsquigarrow$ If you have time, add these filters in front of the $10\,\mathrm{nm}$ wide filters and repeat the HOM dip measurements.

$\rightsquigarrow$ Measure the new width of the HOM dip.

Q15 Compare it with the new energy difference of the photons detected using the $5\,\mathrm{nm}$ width filters.

P 4

Second Harmonic Generation in a KDP crystal

In this session, we study the second harmonic generation process in a non-linear crystal (KDP crystal). We will use a pulsed Nd:YAG @ $1064\,\mathrm{nm}$ from laser to produce light @ $532\,\mathrm{nm}$.

Contents

The KDP crystal is a $30\,\mathrm{mm}$ diameter, $5\,\mathrm{mm}$ thick disk. KDP (KH_2PO_4, potassium dihydrogen phosphate) is a birefrigent negative uniaxial crystal. It has been cut so its optical axis is perpendicular to the entrance face. This axis is denoted as Oz.

The crystal axes frame is denoted as (X, Y, Z). The lab axes frame is denotes as (O, x, y, z). Oz is the propagation direction of the different waves.

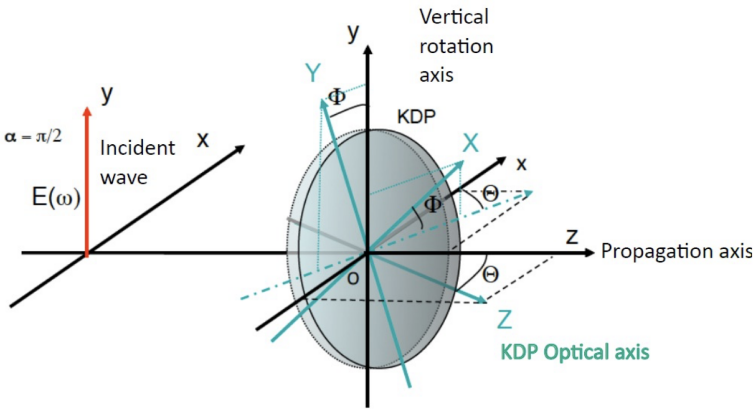

Figure 4.1: Sketch of the crystal(the crystal is a disk). The crystal axes frame is (OX, Y, Z). Θ is the crystal rotation angle around Oy (vertical axis of the mount), Φ is the rotation angle around OZ (crystal optical axis)

Several mechanical settings allow one to move the crystal:

- The KDP disk can be rotated around the vertical axis (Oy). This will adjust the angle Θ between the incident beam (Oz) and the optical axis (OZ). This angle Θ is the phase-matching angle.
- It can also be rotated around its own axis OZ in order to modify the azimuth angle Φ.

The `Nd:YAG` laser is horizontally, linearly polarized. A half wave plate is used to rotate the incident polarization direction on the crystal. The angle α measures the angle between this direction with respect to the vertical axis. In our configuration, the incidence plane will always be defined by Oz and OZ : it is horizontal. The extraordinary direction of polarization is given by the projection of the crystal optical axis (OZ) on the plane wavefront : the extraordinary direction of polarization is then also horizontal. Therefore, the neutral axes will not be affected by a rotation around OZ and a modification of the azimuth angle Φ.

The complete setup provides us with an easy access to three degrees of freedom in order to study SHG:

- the type I and type II phase matching conditions (angle Θ)
- the influence of the crystal orientation (angle Φ)
- the influence of the pump beam polarization (angle α).

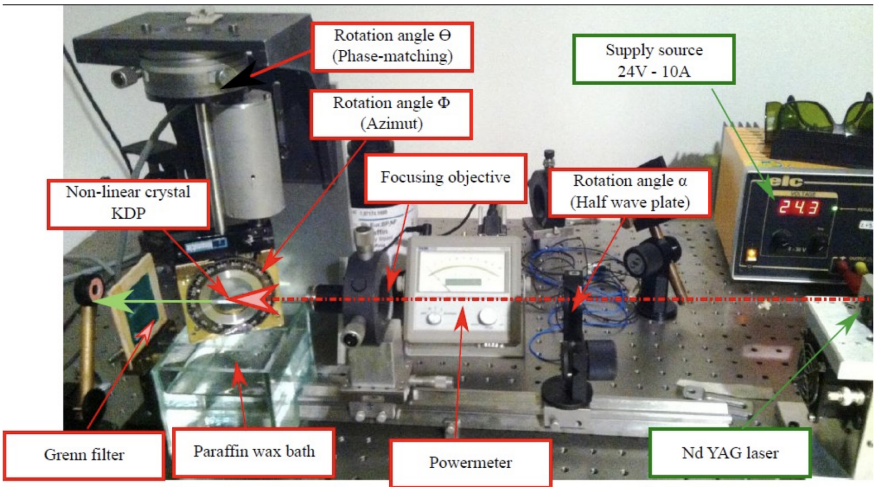

Figure 4.2: Picture of the setup

1 Type I phase matching

subsectionTheoretical study Two conditions must be fulfilled by a non-linear process : energy conservation and momentum conservation. In the specific case of SHG, the momentum conservation can be written :

$$\overrightarrow{k}_{2\omega} = \overrightarrow{k}_{\omega} + \overrightarrow{k}_{\omega}$$

where ω is the angular frequency of the fundamental wave and 2ω, the frequency doubled wave angular frequency. This relation is commonly known as the phase matching condition. For now, we study type I collinear phase matching , meaning that both incident fundamental wave vectors are the same.

Q1 KDP is a negative uniaxial crystal. Show that the type I phase matching condition can be expressed as:

$$n_{e,2\omega}(\Theta) = n_{o,\omega}$$

where $n_{e,2\omega}(\Theta)$ is the extraordinary optical index as seen by a frequency doubled wave that propagates with an angle Θ with respect to the optical axis.

Q2 Use Figure 4.3 to propose a method to determine experimentally the phase matching angle Θ.

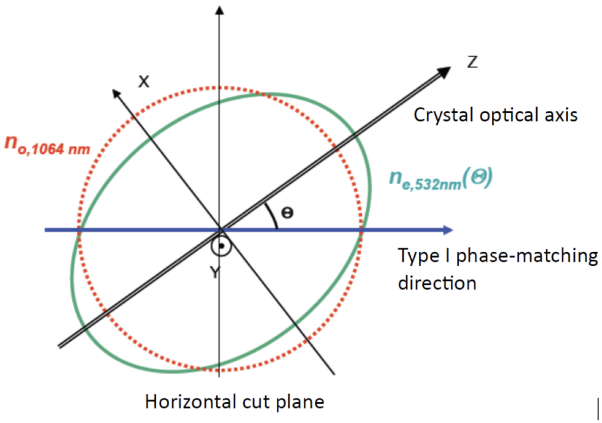

Figure 4.3: Index surfaces in the KDP in the (horizontal) incidence plane.Type I phase-matching

This angle can also be computed from the values of the extraordinary and ordinary indices given by the following Sellmeier equations:

$$n_o^2(\lambda) = 2.25976 + \frac{0.01008956\lambda^2}{\lambda^2 - 0.01294625} + \frac{13.00522\lambda^2}{\lambda^2 - 400}$$

$$n_e^2(\lambda) = 2.132668 + \frac{0.08637494\lambda^2}{\lambda^2 - 0.012281043} + \frac{3.227994\lambda^2}{\lambda^2 - 400}$$

The KDP crystal is a uniaxial negative crystal. We give the following values for the optical indices:

$$n_o(1064) = 1,49384 \qquad n_e(1064) = 1,45985$$
$$n_o(532) = 1,51242 \qquad n_e(532) = 1,47041$$

Use the index surface equation to show that the extraordinary index for a wave propagating with an angle Θ can be deduced from the relation:

$$\frac{1}{n_{e,2\omega}^2(\Theta)} = \frac{\sin^2(\Theta)}{n_{e,2\omega}^2} + \frac{\cos^2(\Theta)}{n_{o,2\omega}^2}$$

Q3 Give an expression for the type I phase matching angle Θ_I as a function of the ordinary and extraordinary optical indices

2 Experimental study of type I phase matching

Be careful ! The pump laser emits an invisible IR beam at $1.064\,\mu\mathrm{m}$, and its average optical power can be set as high as $100\,\mathrm{mW}$. The pulse duration is

$400\,\mathrm{ps}$, meaning the peak power during the pulses reach $250\,\mathrm{kW}$. The repetition rate of the laser can be adjusted between 0 and $1\,\mathrm{kHz}$.

- Always wear safety goggles (type B).
- When not using it, please use the shutter to close the output of the laser.

Please manipulate all components with care, including the paraffin wax filled aquarium.

$\rightsquigarrow$ First, switch on the laser.

- Switch on the supply at $20\,\mathrm{V}$ and $10\,\mathrm{A}$ (button on the right)
- Switch on the pulse generator : set the period of the pulses around $14\,\mathrm{ms}$. This choice for the period will prevent residual absorption in the paraffin wax and any subsequent therml effects.
- Switch on the laser itself (On switch on the side, then in front of the system (push twice this last button).
- Open the mechanical shutter (and remember to close it as soon as you do not use the laser).
- Check the output beam with the IR detection card.

Paraffin wax bath. The crystal is immersed in an immersion oil, with an optical index very close from the optical index of the KDP (paraffin wax optical index$n = 1,47$). Therefore, the fundamental beam is not deviated when propagating through the interface (see Fig 4.4) The crystal rotation angle around Oy is then directly linked to the angle between the pump beam and the crystal optical axis of the KDP.

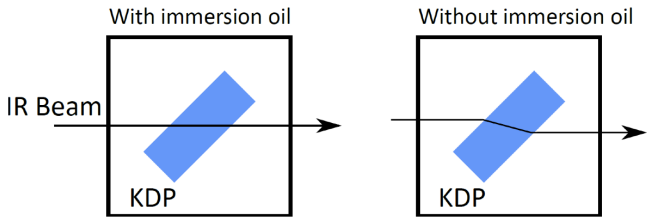

Figure 4.4: Deviation of the IR beam in the crystal when the KDP crystal is or is not immersed in the paraffin wax bath.

$\rightsquigarrow$ Crystal position :

- Set the axes (X, Y) of the crystal at $\Phi = 45^\circ$ with respect to the vertical direction (we will explain later what this configuration is chosen here).
- Move the crystal rotation stage Oy at 45° with respect to the normal incidence.
- Move slightly the crystal around this position in order to observe a green beam. You will probably observe first fringes with the green beam. By adjusting the crystal position, make those fringes disappear. The crystal is then in the correct position.

Q4 Explain the physical origin of the fringes.

$\rightsquigarrow$ Now adjust the position of the focusing objective in order to maximize the green beam intensity.

$\rightsquigarrow$ Same with the half wave plate orientations

$\rightsquigarrow$ ...and finally, same with the angle Φ

$\rightsquigarrow$ Check the green beam polarization direction with respect to the axis $Oxyz$ with an analyzer, and confront this observation to the theoretical predictions.

2.1 Experimental measure of the phase matching angle

As seen on figure 4.3, there are two valid directions corresponding to the phase matching angle. Both are symmetric with respect to the optical axis of the crystal.

$\rightsquigarrow$ You will successively measure those two angular positions in order to get a better precision on your measurement.

Q5 Give an experimental value for the phase matching angle, with its uncertainty, and compare it with the theoretical predictions.

2.2 Influence of the azimuth angle Φ

For the KDP in type I phase matching, we can show that the non-linear polarization of interest in our problem can be expressed as :

$$\mathrm{P}_x^{\mathrm{NL}}(2\omega) = \varepsilon_0 \chi_{\mathrm{eff}}^{(2)} E_y^2(\omega)$$

with $\chi_{\mathrm{eff}}^{(2)}(2\omega, \omega, \omega) = 2d_{36}\sin(\Theta)\sin(2\Phi)$.

In the weak depletion regime, the power of the frequency-doubled beam $P_{2\omega}$ (expressed in watts) is proportional to:

$$P_{2\omega} = K\left(\chi_{\mathrm{eff}}^{(2)}\right)^2 P_\omega^2$$

where P_ω is the power of the fundamental beam (polarized along Oy). K is a proportionality coefficient that is a function of the optical indices, and of other parameters in the experiment (crystal length, waist of the fundamental beam...).

In the previous equation, Θ s set by the phase matching conditions. However, Φ can be still be modified, independently of Θ .

$\rightsquigarrow$ By using a powermeter (with a green beam on the path of the beam), measure the optical power @ $532\,\mathrm{nm}$ as a function of angle Φ. You will have to readjust the angle Θ for each position of Φ, as the rotation axis of the stage is not exactly the optical axis. You will also have to remove the contribution of the stray light to the measured power. You can extinguish the green beam, either by rotating the incident polarization with the half wave plate, or by matching the condition $\sin(2\Phi) = 0$

$\rightsquigarrow$ Plot $P_{2\omega} = f(\Phi)$.

Q6 Comment on the observed behavior.

2.3 Influence of the incident polarization

The type I phase-matching conditions are only fulfilled by the component of the field @$1064\,\mathrm{nm}$ that is ordinary polarized (along the Oy axis of the setup). If the polarization is rotated by an angle α with respect to Oy, one must consider the projection on this axis:

$$E_y(\omega) = E_{\text{incident}}(\omega)\cos\alpha$$

The useful part of the fundamental beam power is thus:

$$P_{\omega,Oy} = P_\omega \cos^2\alpha.$$

$\rightsquigarrow$ Use the powermeter to measure $P_{2\omega} = f(\alpha)$ and plot the corresponding curve.

Q7 Comment on the observed behavior.

2.4 Angular acceptance

$\rightsquigarrow$ Use the camera to observe the light beam spots on the wall, at the output of the setup. The camera can see radiation @$1064\,\mathrm{nm}$, so you can compare both wavelengths spots.

$\rightsquigarrow$ **Be careful, and never place the camera directly in the beam!**

In presence of a phase mismatch Δk, the optical power of the frequency doubled beam follows a sinc^2 behavior with respect to the phase mismatch :

$$P_{2\omega} \propto \left(\frac{\sin \frac{\Delta k l}{2}}{\frac{\Delta k l}{2}} \right)^2$$

Q8 Give the expression of Δk as a function of the refractive indices in the case where we are close to the type I phase matching condition (i.e. for $\Theta \sim \Theta_{\mathrm{I}}$).

Q9 Explain the slight ellipsoidal shape of the frequency doubled beam spot.

$\rightsquigarrow$ Evaluate the divergence of the green beam along its smaller dimension by measuring the lateral size of the beam along its propagation direction with a screen (sheet of paper).

Q10 Deduce an estimation of the angular acceptance and compare to the theoretical value: $3,7\,\mathrm{mrad.\,cm}$.

3 Type II phase matching

3.1 Theoretical study

For type II phase matching, the momentum conservation can be expressed as:

$$\overrightarrow{k}_{2\omega} = \overrightarrow{k}^{o}_{\omega} + \overrightarrow{k}^{e}_{\omega}$$

The two fundamental photons have orthogonal polarizations.

Q11 Explain how to achieve type II phase matching with one single linearly polarized fundamental laser.

Q12 The KDP is a negative uniaxial crystal, show that the type II phase matching condition is given by:

$$n_{e,2\omega}(\Theta) = \frac{1}{2}\left(n_{o,\omega} + n_{e,\omega}(\Theta)\right).$$

You could use the same method as previously in order to get angle Θ . Do not do it again during the session. We get a theoretical value: $\Theta_{\text{II}} = 59^{\circ}$.

We now turn our attention back to the sensitivity of second-harmonic generation to the case of a slight deviation Δk to the phase matching condition.

Q13 Using the same analysis as in the previous section, give the expression of Δk as a function of the refractive indices when close to the type II phase-matching condition ($\Theta \sim \Theta_{\text{II}}$).

Q14 Use figure 4.5 to show that the angular acceptance is better in type II phase-matching than with type I phase-matching.

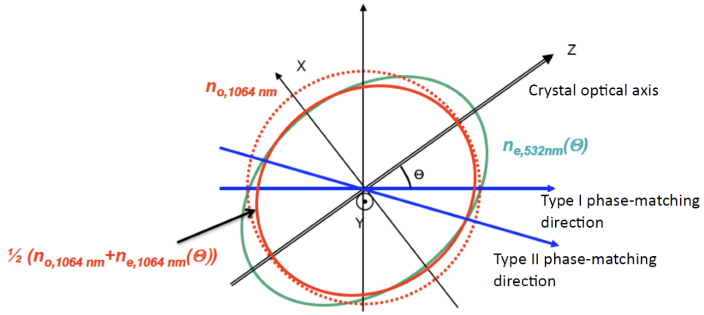

Figure 4.5: Index surfaces in the KDP in the (horizontal) incidence plane. Type II phase-matching compared to type I phase-matching.

4 Experimental study of Type II phase matching

To find the type II phase matching condition, the fundamental polarization should ideally be oriented at 45° with respect to the neutral axis of the crystal.

Q15 By which angle do you have to rotate the half wave plate between the optimal configuration for type I phase matching and type II phase matching?

$\rightsquigarrow$ Compare the shape of the green output beam for type II phase matching to the previously obtained shape for type I phase-matching.

Q16 Explain the differences.

$\rightsquigarrow$ Use an analyzer to give the polarization direction of the output beam with respect to the $Oxyz$ axes.

Q17 Compare this result to your theoretical predictions.

4.1 Phase matching angle measurement

$\rightsquigarrow$ Use the same method as for type I phase matching, and give an experimental measure of the type II phase-matching angle with its associated uncertainty.

Q18 Check if this result is valid according to your theoretical predictions.

4.2 Influence of the azimuth angle Φ.

For type II phase-matching, we can show (see Appendix) that the non-linear polarization of interest can be expressed as:

$$P^{\mathrm{NL}}(2\omega) = \varepsilon_0(d_{14} + d_{36})E_x(\omega)E_y(\omega)\sin(2\Theta)\cos(2\Phi)$$

$\rightsquigarrow$ Use the powermeter to measure the optical power of the frequency doubled beam as a function of the angle Φ. Plot this power $P_{2\omega}$ as a function of Φ.

Q19 Comment your observations. Superimpose both plots for type I and type II phase-matching to comment on the differences between both situations.

4.3 Influence of the incident polarization

α is the angle between the fundamental laser polarization direction and the reference Oy direction.

$\rightsquigarrow$ Use the powermeter and plot $P_{2\omega} = f(\alpha)$.

Q20 Comment and superimpose both plots for type I and type II phase-matching to comment on the differences between both situations.

4.4 Comparing the powers for type I and type II phase-matching.

Q21 Give the maximal output power for the green beams for both type I and type II phase-matching. Comment on the differences predicted by the theoretical considerations in the appendices (you can use the ratio of output optical powers between type I and type II phase-matching).

Appendix 1 : Type I non-linearity

The observed non-linear process is related to a second order induced non-linear polarization. In order to understand more precisely the influence of angles θ_i, α et Φ on this non-linear polarization, one needs to study the second order non-linear susceptibility tensor, $\chi^{(2)}$.

We recall that the induces linear polarization can be written as :

$$\vec{P}(\omega) = \varepsilon_0 \chi^{(1)}(\omega)\vec{E}(\omega)$$

For high power densities, second order, third order and higher order terms can add to the linear polarization term. For second harmonic generation, the term is related to the second order non-linear polarization :

$$P_i^{NL}(2\omega) = \varepsilon_0 \sum_{j,k} \chi_{i,j,k}^{(2)} E_j(\omega) E_k(\omega)$$

where i,j,k correspond to the crystal axes X,Y,Z.

The second order non-linear susceptibility, is a tensor of rank 3 with 3^3=27 components. For low absorption regimes and far from resonances, the tensor can be simplified with only 18 components remaining.

Moreover, when the Kleinman symmetry condition is fulfilled, (or for the specific case of SHG), the second order susceptibility tensor can be reduced to a contracted expression, by using the d_{il} coefficients :

$$d_{ijk} = \frac{1}{2}\chi_{ijk}^{(2)} = d_{il}$$

The last two indices can be reduced to one single index using the following rule :

Axes du cristal	XX	YY	ZZ	YZ ou ZY	XY ou YX	XY ou YX
jk	11	22	33	23 ou 32	13 ou 31	12 ou 21
l	1	2	3	4	5	6

The tensor can then be expressed as a 6x3 matrix, containing 18 elements :

$$d_{il} = \begin{bmatrix} d_{11} & d_{12} & d_{13} & d_{14} & d_{15} & d_{16} \\ d_{21} & d_{22} & d_{23} & d_{24} & d_{25} & d_{26} \\ d_{31} & d_{32} & d_{33} & d_{34} & d_{35} & d_{36} \end{bmatrix}$$

The KDP crystal under study in this labwork session belongs to the tetragonal symmetry group $\bar{4}2m$,. The contracted susceptibility tensor has only 3 non-zero elements remaining :

$$d_{il} = \begin{bmatrix} 0 & 0 & 0 & d_{14} & 0 & 0 \\ 0 & 0 & 0 & 0 & d_{25} & 0 \\ 0 & 0 & 0 & 0 & 0 & d_{36} \end{bmatrix}$$

With $d_{14} = d_{25}$, and $d_{14} = 0{,}39$ pm.V^{-1} and $d_{36} = 0{,}43$ pm.V^{-1}.

In the crystal axis frame (O, X, Y, Z) :

$$P_i^{NL}(2\omega) = \varepsilon_0 \sum_{j,k} \chi^{(2)}_{i,j,k} E_j(\omega) E_k(\omega)$$

Is given by :

$$\begin{pmatrix} P_X(2\omega) \\ P_Y(2\omega) \\ P_Z(2\omega) \end{pmatrix} = 2\varepsilon_0 \begin{pmatrix} 0 & 0 & 0 & d_{14} & 0 & 0 \\ 0 & 0 & 0 & 0 & d_{14} & 0 \\ 0 & 0 & 0 & 0 & 0 & d_{36} \end{pmatrix} \begin{pmatrix} E_X^2(\omega) \\ E_Y^2(\omega) \\ E_Z^2(\omega) \\ 2E_Y(\omega)E_Z(\omega) \\ 2E_X(\omega)E_Z(\omega) \\ 2E_X(\omega)E_Y(\omega) \end{pmatrix}$$

so : $P_i^{NL}(2\omega) = \varepsilon_0 \sum_{j,k} \chi^{(2)}_{i,j,k} E_j(\omega) E_k(\omega)$

$$\begin{pmatrix} P_X(2\omega) \\ P_Y(2\omega) \\ P_Z(2\omega) \end{pmatrix} = 4\varepsilon_0 \begin{pmatrix} d_{14}E_Y(\omega)E_Z(\omega) \\ d_{14}E_X(\omega)E_Z(\omega) \\ d_{36}E_X(\omega)E_Y(\omega) \end{pmatrix}$$

Fo a type I phase-matching in KDP, the incident wave is necessarily ordinary polarized, meaning its projection on the optical axis OZ is zero. There is only one term contributing to the frequency doubled beam :

$$P_Z^{NL}(2\omega) = \varepsilon_0 \chi^{(2)}_{Z,X,Y} E_X(\omega) E_Y(\omega) + \varepsilon_0 \chi^{(2)}_{Z,Y,X} E_X(\omega) E_Y(\omega)$$

$$P_Z^{NL}(2\omega) = 2\varepsilon_0 \chi^{(2)}_{Z,X,Y} E_X(\omega) E_Y(\omega) = 4\varepsilon_0 d_{36} E_X(\omega) E_Y(\omega)$$

Moreover, In this configuration, the output beam is extraordinary polarized. The induced non-linear polarization must then be projected onto the direction (Ox).

We get : $P_x^{NL}(2\omega) = \varepsilon_0 \chi^{(2)}_{eff} E_y^{\,2}(\omega)$ with $\chi^{(2)}_{(eff,o,o)}(2\omega,\omega,\omega) = 2d_{36}\sin(\Theta)\sin(2\Phi)$, the effective non-linear permittivity in type I phase-matching

Appendix 2 : Type II non-linearity

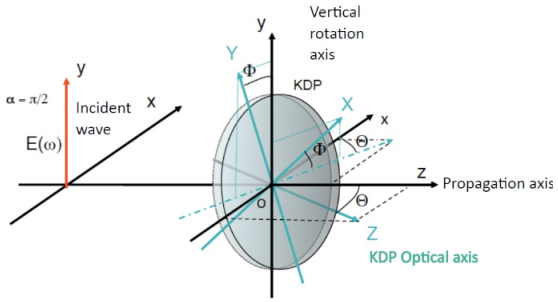

In the crystal axes frame (O,X,Y,Z), the non-linear polarization writes :

$$P_i^{NL}(2\omega) = \varepsilon_0 \sum_{j,k} \chi^{(2)}_{i,j,k} E_j(\omega) E_k(\omega)$$

So :

$$\begin{pmatrix} P_X(2\omega) \\ P_Y(2\omega) \\ P_Z(2\omega) \end{pmatrix} = 2\varepsilon_0 \begin{pmatrix} 0 & 0 & 0 & d_{14} & 0 & 0 \\ 0 & 0 & 0 & 0 & d_{14} & 0 \\ 0 & 0 & 0 & 0 & 0 & d_{36} \end{pmatrix} \begin{pmatrix} E_X^2(\omega) \\ E_Y^2(\omega) \\ E_Z^2(\omega) \\ 2E_Y(\omega)E_Z(\omega) \\ 2E_X(\omega)E_Z(\omega) \\ 2E_X(\omega)E_Y(\omega) \end{pmatrix}$$

$$\begin{pmatrix} P_X(2w) \\ P_Y(2w) \\ P_Z(2w) \end{pmatrix} = 4\varepsilon_0 \begin{pmatrix} d_{14}E_Y(w)E_Z(w) \\ d_{14}E_X(w)E_Z(w) \\ d_{36}E_X(w)E_Y(w) \end{pmatrix}$$

In type II phase-matching, the incident wave has two components : the ordinary component along (Oy) and the extraordinary component along (Ox). The output beam is an extraordinary wave (polarized along Ox).
First, one has to write the components of the incident wave in the crystal axes frame, and then project the polarization on the Ox direction.

E_X, E_Y, E_Z can be writen as functions of de E_x, E_y, E_z :

$$E_X = E_x \cos(\Theta)\cos(\Phi) + E_y \sin(\Phi) + E_z \cos(\Phi)\sin(\Theta)$$
$$E_Y = -E_x \cos(\Theta)\sin(\Phi) + E_y \cos(\Phi) - E_z \sin(\Phi)\sin(\Theta)$$
$$E_Z = -E_x \sin(\Theta) + E_z \cos(\Theta)$$

$E_z = 0$ then :

$$E_X = E_x \cos(\Theta)\cos(\Phi) + E_y \sin(\Phi)$$
$$E_Y = -E_x \cos(\Theta)\sin(\Phi) + E_y \cos(\Phi)$$
$$E_Z = -E_x \sin(\Theta)$$

$$\begin{pmatrix} P_X(2w) \\ P_Y(2w) \\ P_Z(2w) \end{pmatrix} = 4\varepsilon_0 \begin{pmatrix} d_{14}E_Y(w)E_Z(w) \\ d_{14}E_X(w)E_Z(w) \\ d_{36}E_X(w)E_Y(w) \end{pmatrix}$$

$$= 2\varepsilon_0 \begin{pmatrix} d_{14}E_xE_x \sin(2\Theta)\sin(\Phi) - d_{14}E_xE_y \sin(\Theta)\cos(\Phi) \\ -d_{14}E_xE_x \sin(2\Theta)\cos(\Phi) - d_{14}E_xE_y \sin(\Theta)\sin(\Phi) \\ -d_{36}E_xE_x \cos^2(\Theta)\sin(2\Phi) + d_{36}E_yE_y \sin(2\Phi) + d_{36}E_xE_y \cos(\Theta)\cos(2\Phi) \end{pmatrix}$$

We know that Ex is an ordinary wave and Ey is an extraordinary wave, so the terms ExEx = EyEy do not contribute efficiently to the SHG process for a type II phase-matching. The remaining contributions are :

$$\begin{pmatrix} P_X(2w) \\ P_Y(2w) \\ P_Z(2w) \end{pmatrix} = 4\varepsilon_0 \begin{pmatrix} d_{14}E_Y(w)E_Z(w) \\ d_{14}E_X(w)E_Z(w) \\ d_{36}E_X(w)E_Y(w) \end{pmatrix} = 2\varepsilon_0 \begin{pmatrix} -d_{14}E_xE_y \sin(\Theta)\cos(\Phi) \\ -d_{14}E_xE_y \sin(\Theta)\sin(\Phi) \\ d_{36}E_xE_y \cos(\Theta)\cos(2\Phi) \end{pmatrix}$$

Finally, one has to project those components onto the direction Ox.

$$P_x = P_X \cos(\Theta)\cos(\Phi) - P_Y \cos(\Theta)\sin(\Phi) - P_Z \sin(\Theta)$$

We get : $P_x(2\omega) = \varepsilon_0(d_{14} + d_{36})E_x(\omega)E_y(\omega)\sin(2\Theta)\cos(2\Phi)$

P 5

Spectroscopy of a jet of atoms

This lab illustrates the first stage of laser atom cooling experiments, namely the production of a jet of atoms from an oven, which will then be captured in a magneto-optical trap. You will carry out spectroscopy of the jet of atoms using a laser, most specifically the absorption and fluorescence spectroscopy of a line of the hyperfine structure of rubidium 85 around $780\,\mathrm{nm}$.

Contents

P1 Fluorescence rate of a two-level atom.
In this tutorial, atoms will be modelled as two-level systems. The interaction between a laser beam and a two-level atom is described by the optical Bloch equations (OBE). The stationary solution of the OBEs for the fraction of atoms in the excited state is given by

$$\Pi_e = \frac{1}{2}\frac{s}{1+s}\ , \tag{5.1}$$

where the saturation parameter writes

$$s = \frac{I/I_s}{1+4\Delta^2/\Gamma^2}\ , \tag{5.2}$$

as a function of the laser detuning to the atomic transition

$$\Delta = (\omega - \omega_0) - \mathbf{k} \cdot \mathbf{v} \ . \tag{5.3}$$

The fraction of atoms in the ground state is simply deduced from that in the excited state:

$$\Pi_g = 1 - \Pi_e. \tag{5.4}$$

In the equations above, we have used the following notations:

- ω, I and $\mathbf{k}$ are respectively the pulsation of the laser beam, its intensity and its wave vector;
- ω_0, I_s and $1/\Gamma$ are respectively the Bohr pulsation of the atomic transition, its saturation intensity and the lifetime of the excited state.
- $\mathbf{v}$ is the velocity of the atom in the laboratory reference frame.

Finally, remember that the fluorescence rate of a two-level atom is equal to $\Pi_e\Gamma$.

Q22 Name the function representing the fluorescence spectrum of an atom, i.e. the change in fluorescence rate as a function of detuning. Determine its total width at half-maximum in the low-intensity limit. $I \ll I_s$.

Q23 Explain why the fluorescence and absorption spectra of the laser by an atom have an identical profile as a function of the laser detuning.

Q24 What effect causes the term $-\mathbf{k} \cdot \mathbf{v}$ in the expression of the detuning Δ (Equation 5.3) ?

Q25 In a gas at equilibrium at a temperature T, the fluorescence spectrum broadened by the Doppler effect has a total width at half-maximum equal to

$$\Delta\omega = \sqrt{8\ln 2}\,\sqrt{\frac{k_B T}{m}}\,\frac{\omega_0}{c}. \tag{5.5}$$

In this equation, $k_B = 1.38 \times 10^{-23}$J/K is Boltzmann's constant, $m = 1.41 \times 10^{-25}$ kg is the mass of a rubidium atom and c is the speed of light in vacuum. Calculate the Doppler shift expected in a cell at room temperature ($T \sim 20°$C) for the rubidium line centred at $780\,\mathrm{nm}$.

P2 Distribution of velocities in the jet of atoms.
The jet of atoms is obtained from a rubidium vapour produced by heating a metal sample in an oven to a temperature of $T \simeq 100\,^{\circ}\mathrm{C}$. This vapour escapes from the oven through a first circular orifice of diameter $D_1 = 5\,\mathrm{mm}$. A second orifice of diameter $D_2 = 1\,\mathrm{cm}$ placed at a distance $L \simeq 20\,\mathrm{cm}$ from the first one filters the distribution of transverse velocities, thus creating an atomic jet.

Q26 Assuming that the gas is at thermodynamic equilibrium in the oven, give the energy distribution of the atoms, then their velocity distribution, expressed as a function of the norm of the velocity vector $v = \|\mathbf{v}\|$.

Q27 Estimate numerically the average $\langle v \rangle = \sqrt{9\pi k_B T/8m}$ of the norm of the velocity vector at the exit of the oven.

Q28 Assuming that the velocity of an atom along the axis of the circular orifices is equal to $\langle v \rangle$, estimate the maximum transverse velocity that will allow this atom to reach the last chamber. To make the calculation easier, consider that $D1 = D2 = 1\,\mathrm{cm}$.

1 Absorption spectrum

In this section you will first measure the absorption spectrum of a laser beam of wavelength $780\,\mathrm{nm}$ through a spectroscopy cell at room temperature, then through the jet of atoms produced by the oven. The optical set-up is shown in figure 5.1 below.

The natural abundance of the two isotopes of Rubidium is $\sim 72.2\%$ for the 85 isotope and $\sim 27.8\%$ for the 87 isotope..

IMPORTANT Make sure the laser diode is set to the following values: selected current (« set ») $I_{\text{set}} = 143{,}5\,\mathrm{mA}$ and set temperature $T_{\text{set}} = 19{,}550\,^{\circ}\mathrm{C}$.

Absorption spectrum through the cell at room temperature

$\rightsquigarrow$ Scan the laser diode current using the RIGOL function generator connected to the external modulation input of the laser diode controller and display on the oscilloscope 4 resonances such as those shown in figure 5.2. To do this, choose a symmetrical triangular sweep pattern, a modulation frequency of the order of $100\,\mathrm{Hz}$ and a peak-to-peak modulation amplitude of the order of $300\,\mathrm{mV}$ (and a zero offset voltage).

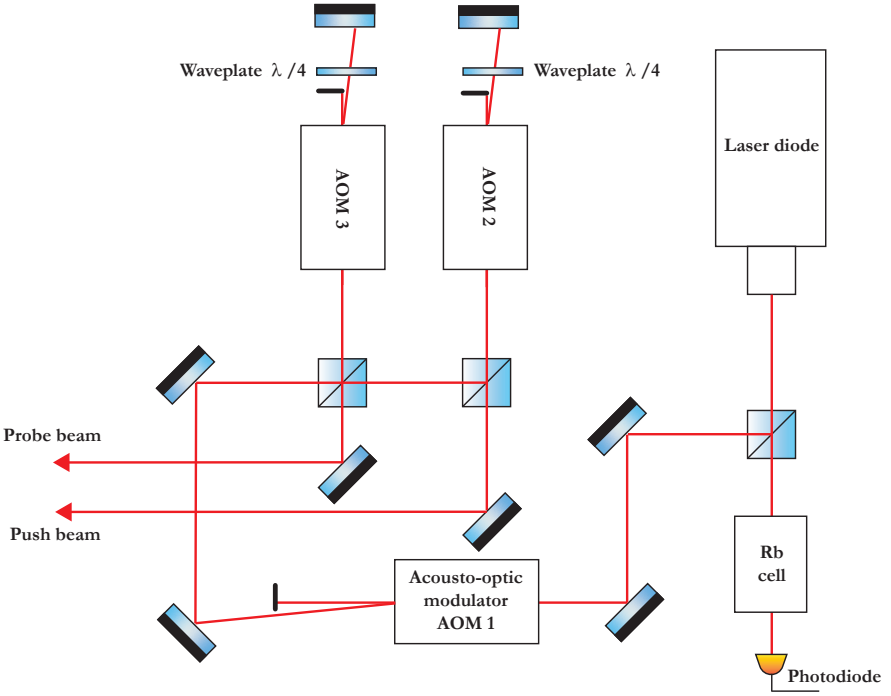

Figure 5.1: Description of the optical table. The light source is a laser diode emitting around $780\,\mathrm{nm}$. Part of the beam is used for spectroscopy in the glass cell. The other part of the beam is sent through a first single-pass AOM. The laser beam is then split into two beams, each injecting a double-pass AOM. The probe and push beams thus generated are sent to the vacuum chamber.

Each of these resonances actually comprises several unresolved atomic transitions: the difference in energy between the hyperfine sub-states of the excited state is smaller than the Doppler shift at ambient temperature.
An energy diagram of the hyperfine structure of rubidium isotopes 85 and 87 is given in the appendix.

Q29 The lines observed in Figure 3 are identified through the isotope (85 or 87) and the F hyperfine state of the ground state. Justify this identification by checking that the relative distance between the two lines of each isotope

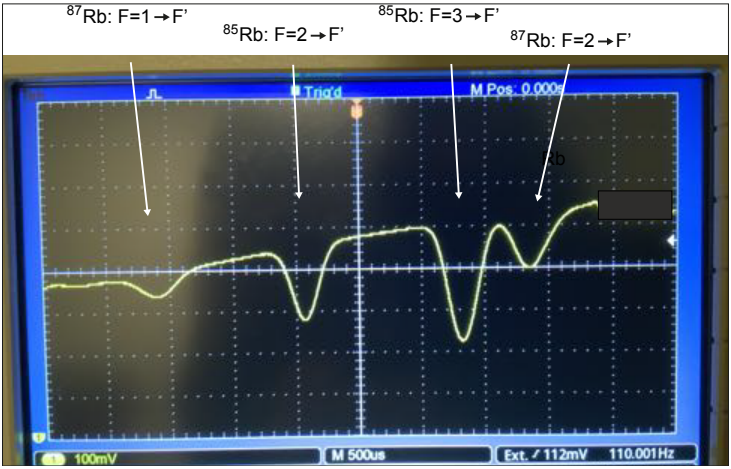

Figure 5.2: Absorption spectrum in the cell. This spectrum was obtained using the same set-up as the one you have, by measuring the laser intensity transmitted through the cell using an amplified photodiode and sweeping the frequency of the laser diode. It shows 4 lines linked to the hyperfine structure of the 85 and 87 isotopes of rubidium around $780\,\mathrm{nm}$ (see the energy diagrams in the appendix).

corresponds to what is expected from the energy diagrams.

Q30 Using the same data, determine the coefficient of proportionality between the current modulation voltage and the optical frequency of the laser.

Q31 Measure the total width at half-maximum of the two rubidium 85 resonances. Compare your result with the natural width expected for a transition, i.e. $\Gamma/2\pi = 6{,}1\,\mathrm{MHz}$, and with the width calculated in question Q4.
Comment your result.

Absorption spectrum through the jet of atoms In this section, you will measure the absorption spectrum of a jet of rubidium atoms using the probe beam shown in figure 5.3.

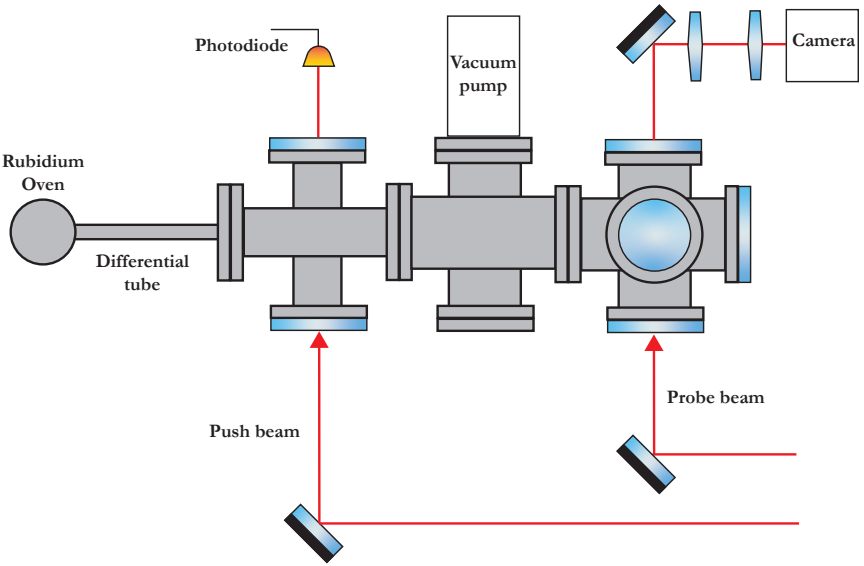

Figure 5.3: Description of the vacuum chamber. The jet of rubidium atoms is produced in an oven heated to around $100\,°\mathrm{C}$ and whose outlet is bounded by a narrow cylinder. The jet propagates from left to right in the diagram. The transverse velocity distribution of the jet is characterised in the rightmost chamber, either by absorption of the probe beam using a photodiode (not shown), or by fluorescence induced by the same probe beam using a camera. In the intermediate chamber, a push beam can deflect the atomic beam before it reaches the probe.

Initial settings. The AOM2 and AOM3 acousto-optic modulators are driven using the SIGLENT arbitrary function generator, which has two output channels. It will be ensured for both output channels that a sinusoid of frequency $200\,\mathrm{MHz}$ and amplitude $100\,\mathrm{mV}$ is sent to the two acousto-optic modulators.

$\rightsquigarrow$ Simultaneously observe the signals from the photodiodes in the cell and the jet using an oscilloscope.

Q32 What obvious difference(s) can you see between the two absorption signals?

⇝ Modify the amplitude of the laser diode current sweep so that only the most intense absorption line is observed in the cell. The absorption spectrum from the jet of atoms should now look like that shown in figure. 5.4.

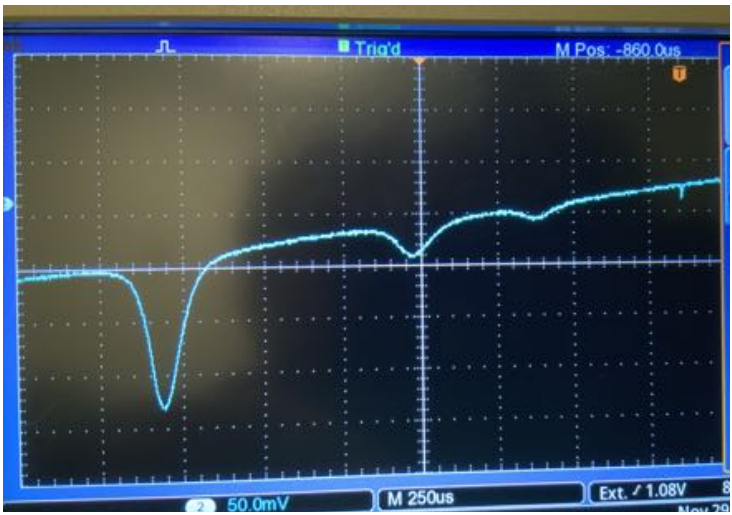

Figure 5.4: Absorption spectrum through the atomic jet. This spectrum was obtained using the same set-up as the one you have, by measuring the laser intensity transmitted through the vacuum chamber and the atomic jet, using an amplified photodiode and sweeping the frequency of the laser diode.

Q33 Using the energy diagrams given in the appendix, identify the atomic transitions visible in the absorption spectrum of the jet of atoms.

Q34 Measure the total width at half-maximum of the most intense absorption line across the jet.
From the expression for Doppler broadening given in equation 5.5, estimate an "effective" temperature corresponding to your linewidth measurement. Why can't this be a 'true' temperature?

Q35 Discuss the value of the atom jet for spectroscopic measurements.

Q36 Give a rough estimate of the frequency resolution achieved by external modulation of the laser diode current.
In the next section, we will see that this resolution limit can be greatly reduced by using an acousto-optic modulator (AOM) to sweep the laser beam frequency.

2 Fluorescence spectrum

You are now going to observe the fluorescence spectrum of the atomic jet using a camera positioned perpendicular to the probe beam.

$\rightsquigarrow$ Using modulation of the laser diode current to vary the frequency of the laser beam (procedure identical to the previous section), observe the fluorescence resonance on the camera.

Q37 Determine the orientation of the probe beam and the jet of atoms on the camera image.

$\rightsquigarrow$ Disable the laser diode current sweep and add a $50\,\Omega$ termination to the controller's external modulation input. Slowly modify (a few MHz at a time) the frequency of AOM No. 3 driven by the SIGLENT generator until the fluorescence resonance on the camera is restored.

$\rightsquigarrow$ Determine the frequency range that needs to be covered to visualise the entire fluorescence resonance, i.e. the minimum (respectively maximum) frequency below (respectively above) which the fluorescence signal is negligible.

Q38 What is the first observation you can make about the resolution of the frequency sweep performed using the AOM compared with that performed by modulating the laser diode current?

$\rightsquigarrow$ We want to measure the shape of the observed resonance precisely. To begin, acquire a fluorescence image using the camera control software. Elect an area of interest (ROI) covering the entire sensor in the direction of the laser beam but only the fluorescence signal in the direction of the jet. Extract the average number of grey levels $N_{\text{n.g.}}$ calculated by the histogram function.

$\rightsquigarrow$ We also want to ensure that we are working within a linear response regime, defined by a saturation parameter s less than the unit.
To determine this regime in the experiment, we begin by choosing the AOM frequency for which the fluorescence signal (i.e. the average number of grey

levels $N_{\text{n.g.}}$ in the ROI) is maximum. Keeping this frequency fixed, we vary the amplitude of the signal sent to the AOM by the SIGLENT generator: for each value of the amplitude chosen, we measure both $N_{\text{n.g.}}$ and the voltage V_{PD} on the photodiode of the probe beam.

Q39 Plot the curve $N_{\text{n.g.}}$ as a function of V_{PD} and identify the linear and saturated fluorescence regimes. Determine the maximum value of amplitude of the AOM drive signal below which the variation of $N_{\text{n.g.}}$ is linear with V_{PD}.

$\rightsquigarrow$ Measure the number of grey levels in the ROI as a function of the frequency of the AOM drive signal. Choose about ten frequency values spread over the range you determined in question Q16.

Q40 Plot the fluorescence spectrum obtained as a function of the AOM drive frequency. Determine its total width at half-height and compare it with that of the absorption spectrum by the jet of atoms. Be careful to take into account the double passage through the AOM, which shifts the laser beam frequency by twice the AOM drive frequency!

$\rightsquigarrow$ When the drive frequency of the AOM is varied, the diffraction efficiency changes as we move away from the Bragg condition. This effect is likely to alter the measurement of the fluorescence spectrum and can be corrected. To do this, measure V_{PD} as a function of AOM frequency over the range used for the previous measurement in order to calibrate the variation in optical power of the probe beam. Correct the fluorescence spectrum measurement to compensate for the effect of the variation in probe beam power.

Q41 Plot the corrected spectrum and compare it with the raw spectrum. Does it seem necessary to take into account the modulation of the optical power of the probe beam?

$\rightsquigarrow$ Reproduce the measurement of the fluorescence spectrum for the maximum value of the optical power of the probe beam and plot the new spectrum obtained.

Q42 Compare the width of this spectrum with that of the spectrum obtained at low power and comment on the effect of saturation.

3 OPTIONAL SECTION - Mechanical action of light on atoms

If you have time, you can deal with this optional section.

In this final section, we study the mechanical effect of laser light on the atomic jet. This effect is similar to that exerted by sunlight on the tail of a comet: the radiation pressure exerted by the sunlight bends the tail of the comet.

The radiation pressure force exerted by the laser light on the atom at two levels is written,

$$\mathbf{F}_{\text{rad}} = \hbar\mathbf{k}\frac{\Gamma}{2}\frac{s}{1+s} \ . \tag{5.6}$$

$\rightsquigarrow$ Add the pusher beam to the empty chamber at the end of the oven. Set the power of the push beam to its maximum and vary its frequency until an effect on the fluorescence resonance is observed.

Q43 Interpret the modification of the spectrum by the mechanical action of the laser beam at the oven outlet.

Q44 Estimate the variation in impulse experienced by an atom passing through a laser beam.

Q45 Discuss the best beam size for measuring the velocity distribution of the jet of atoms.

4 Annexe

Hyperfine structure of the D2 line of rubidium isotopes 85 and 87. The figures are taken from documents posted online by Daniel Steck at the following address `http://steck.us/alkalidata/`.

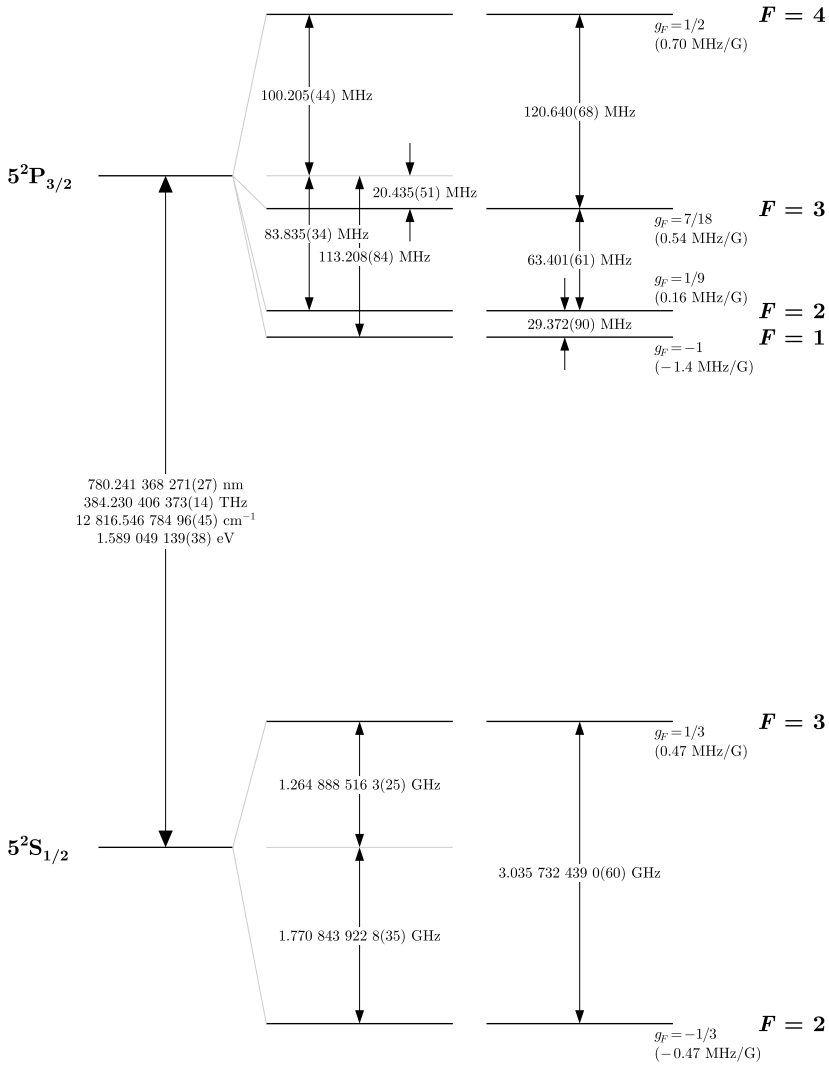

Figure 5.5: Hyperfine structure of the D2 transition of rubidium 85.

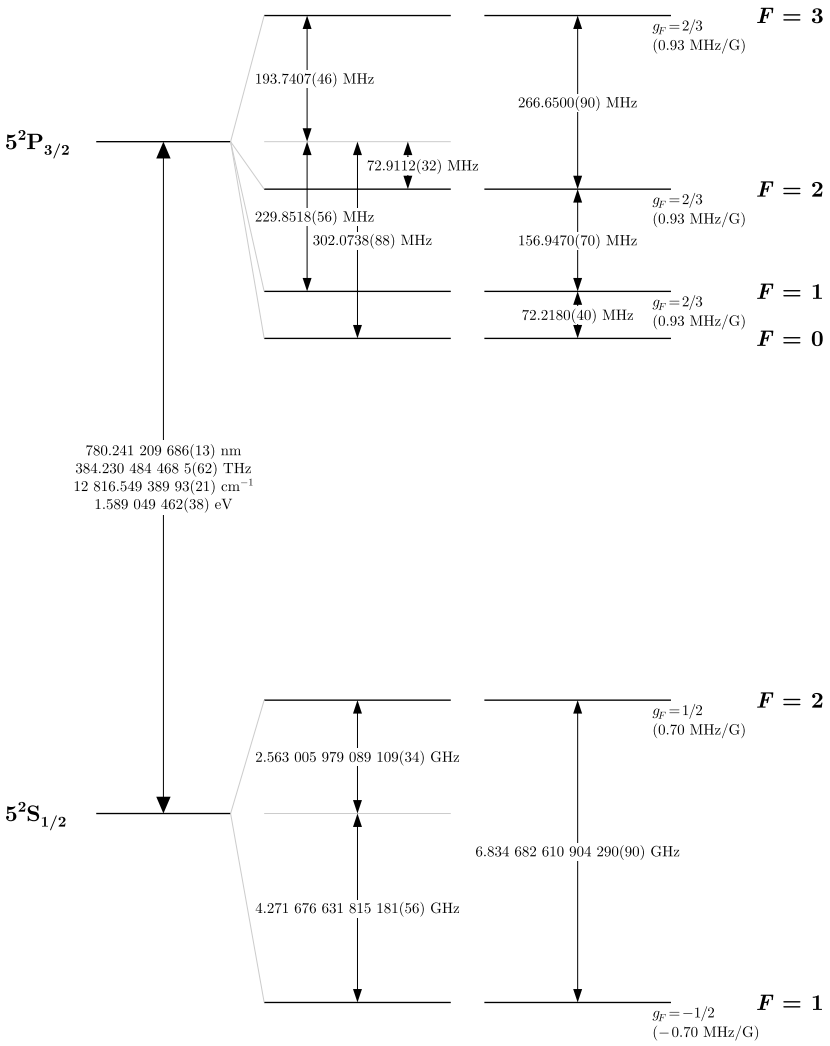

Figure 5.6: Hyperfine structure of the D2 transition of rubidium 87.